FROM THE DEPARTMENT OF ONCOLOGY, RADIOLOGY AND CLINICAL
IMMUNOLOGY, SECTION OF RADIOLOGY,
UPPSALA UNIVERSITY, UPPSALA, SWEDEN

On Contrast-Enhanced Magnetic Resonance Angiography of the Aortoiliac arteries

Johan WIKSTRÖM

Uppsala 2001

Dissertation in Radiology for the Degree of Doctor of Philosophy, Faculty of Medicine, presented at Uppsala University in 2001.

ABSTRACT

Wikström, J. 2001. On Contrast-Enhanced Magnetic Resonance Angiography of the Aortoiliac Arteries. 34 pp Uppsala. ISBN 91-628-4814-3

In contrast-enhanced magnetic resonance angiography (CE-MRA), vascular signal is produced by the acquisition of a T1-weighted magnetic resonance imaging scan while the presence of a contrast agent induces a low T1 in blood. In this thesis, CE-MRA of the aortoiliac arteries was evaluated. Different contrast agents and techniques for synchronisation of the scan with the contrast bolus passage were assessed.

In 30 patients with clinically suspected iliac artery stenoses, contrast-enhanced magnetic resonance angiography was compared with duplex ultrasound scanning and digital subtraction x-ray angiography (DSA), with intraarterial pressure measurements as reference. No statistically significant differences in sensitivity or specificity were observed between the techniques regarding detection of haemodynamically significant iliac stenoses. The use of multiplanar reformats and source images in the MRA examinations was of value for differentiation between high-grade stenoses and occlusions. With DSA as reference method, MRA had significantly higher sensitivity and specificity than duplex for detection of $\geq$50% stenoses.

In 14 patients who underwent iliac artery MRA, differences in contrast arrival time of up to 7 s were observed between the aorta and the common femoral artery. A dual-station timing technique adjusting for this difference was found feasible. Compared with a fluoroscopically triggered technique (n=13), which is used in clinical routine, the dual-station technique was more reliable for the visualisation of distal vessels.

In a clinical phase II study comparing doses of the contrast agent gadobenate dimeglumine from 0.0125-0.2 mmol/kg for enhancement of iliac artery MRA, significant improvement in subjective diagnostic quality compared with time-of-flight (TOF)-MRA was found at all doses from 0.025 mmol/kg. An increasing trend with dose was observed up to a dose of 0.05-0.1 mmol/kg.

In a phase I clinical study on the intravascular iron oxide contrast agent NC100150 Injection, a positive dose response was observed for abdominal vascular enhancement, with the highest contrast-to-noise ratio (CNR) observed at 4.0 mg Fe/kg bw at 1.5 T and at 2.5-4 mg Fe/kg bw at 0.5 T. At 1.5 T higher calculated R2* values were found for the aorta than for the inferior vena cava.

Key words: Magnetic resonance imaging, Magnetic resonance angiography, Contrast media, Arteriosclerosis, Iliac artery, Blood pressures.

Johan Wikström,
Department of Oncology, Radiology and Clinical Immunology, Section of Radiology
Uppsala University Hospital,
S-751 85 Uppsala, Sweden

ISBN 91-628-4814-3

Printed in Sweden by Eklundhofs Grafiska AB, Uppsala 2001

ORIGINAL PAPERS

This thesis is based on the following papers, which will be referred to by their Roman numerals (I-IV).

I. Wikström J, Holmberg A, Johansson L, Löfberg A-M, Smedby Ö, Karacagil S, Ahlström H.: Gadolinium-enhanced magnetic resonance angiography, digital subtraction angiography and duplex of the iliac arteries compared with intra-arterial pressure gradient measurements. Eur J Vasc Endovasc Surg 2000; 19:516-523.

II. Wikström J, Johansson L, Karacagil S, Ahlström H.: On the importance of adjusting for differences in proximal and distal contrast bolus arrival times in contrast-enhanced iliac artery magnetic resonance angiography. (Manuscript)

III. Wikström J, Wasser M, Pattynama P, Hentrich H-R, Daprà M, Kirchin M, Spinazzi A, Ahlström H.: Gadobenate dimeglumine in contrast-enhanced magnetic resonance angiography of the pelvic arteries. (Manuscript)

IV. Wikström J, Johansson L, Ericsson A, Börseth A, Åkeson P, Ahlström H.: Abdominal vessel enhancement with an ultrasmall, superparamagnetic iron oxide blood pool agent: evaluation of dose and echo time dependence at different field strengths. Acad Radiol 1999; 6 (5):292-298.

to Anna-Karin,

Carolina, Johanna and Carl

CONTENT

ABBREVIATIONS

CE-MRA	Contrast-enhanced magnetic resonance angiography
CNR	Contrast-to-noise ratio
CTA	Computed tomography angiography
CV	Coefficient of variation
DSA	Digital subtraction angiography
DUS	Duplex ultrasound scanning
ECG	Electrocardiograph
FOV	Field-of-view
GRE	Gradient echo
IAPM	Intra-arterial pressure measurement
IVC	Inferior vena cava
MIP	Maximum intensity projection
MPR	Multiplanar reformatation
MRA	Magnetic resonance angiography
MRI	Magnetic resonance imaging
NEX	Number of excitations
PC	Phase contrast
PSV	Peak systolic velocity
R1	T1 relaxation rate
R2	T2 relaxation rate
R2*	T2* relaxation rate
r_1	T1 relaxivity
r_2	T2 relaxivity
ROI	Region of interest
SI	Signal intensity
SNR	Signal-to-noise ratio
SPIO	Superparamagnetic iron oxide
SSD	Shaded surface display
T1	Longitudinal or spin-lattice relaxation time
T2	Transverse or spin-spin relaxation time
T2*	Total transverse relaxation time
TE	Echo time
TOF	Time-of-flight
TR	Repetition time
USPIO	Ultrasmall superparamagnetic iron oxide
VRT	Volume rendering technique

On Contrast-Enhanced Magnetic Resonance Angiography of the Aortoiliac arteries

Johan WIKSTRÖM

INTRODUCTION

Atherosclerosis

Atherosclerosis is a generalised disease (1, 2) leading to luminal narrowing, which may result in a decrease in blood flow distal to the lesion (3). This may give rise to clinical symptoms of ischaemia if severe enough. There is also an increased risk for local thromboses, which may occlude the vessel or cause embolic occlusions (4).

Radiological methods such as x-ray angiography, duplex ultrasound scanning, computed tomography angiography (CTA) and magnetic resonance angiography (MRA) are of great importance for the detection and grading of these lesions. In the studies presented in this thesis, contrast-enhanced MRA (CE-MRA) of the aortoiliac arteries is investigated.

X-ray angiography

X-ray angiography, nowadays mostly as digital subtraction angiography (DSA), has been used for vascular imaging for more than half a century(5, 6). It has been the reference method in most vascular territories because of its high resolution and speed, allowing accurate visualisation of lesions and assessments of vascular dynamics. DSA has some disadvantages, however. It involves arterial catheterisation, which carries a risk of local complications (haematoma, dissection, thrombosis or infection) of 7%, and of systemic complications of 1.8% (7). In addition, the patient is exposed to ionising radiation, which involves a small but not negligible risk (8, 9). The contrast agents used for DSA are also potentially nephrotoxic, especially in diabetic patients with already impaired renal function (10). For these reasons, alternative vascular imaging modalities have been developed.

Intra-arterial pressure measurements (IAPM)

The significance of an arterial stenosis lies in the resulting reduction of blood flow distal to the lesion. It has been shown (3) that the blood flow is not reduced until a certain level of stenosis is reached, whereafter the blood flow decreases profoundly. This level of stenosis is dependent on the normal diameter of the vessel and the flow velocity (11). In the iliac arteries the critical diameter reduction is in the order of 50% (11). For these reasons, the significance of an arterial stenosis may be difficult to assess by morphological methods alone (12). The reduction in blood flow is difficult to measure. It is known, however, that the reduction in blood flow distal to a stenosis is related to the pressure drop (or gradient) over the stenosis (3). The pressure gradient can be measured in conjunction with the angiographic procedure (13, 14), and this is regarded as the most reliable technique for detection of a hemodynamically significant lesion (15, 16).

Computed tomography angiography (CTA)

With recent developments in CT technology, the scan times have been greatly reduced, permitting high-resolution arterial phase angiograms to be obtained (17). CTA has been used with promising results in various territories(17-21). It requires no catheterisation, but otherwise carries the same disadvantages as DSA in terms of ionising radiation, and the use of potentially nephrotoxic contrast agents. One difficulty with previously used CTA display methods (maximum intensity projection [MIP], and shaded surface display [SSD]) is that skeletal structures and vessel wall calcifications may obscure the vessel lumen (20). This problem seems to have been solved by the use of post-processing with the volume-rendering technique (VRT), with which overlying high-attenuating structures are interactively rendered

transparent, in order not to obscure the vessel (22).

Duplex ultrasound scanning (DUS)

In duplex ultrasound scanning, B-mode and doppler recording is combined to give both morphological and velocity information. The evaluation is further aided by colour display of moving blood (colour duplex scanning). Sites of vascular narrowing are identified by means of colour duplex, after which the stenosis is graded by doppler measurements. Different doppler criteria for assessing the degree of stenosis have been described. In the iliac arteries, the use of a peak systolic velocity (PSV) ratio has shown highest accuracy for grading of stenoses (23). This ratio is defined as the quotient between the PSV at the stenosis and the PSV in the adjacent normal part of the vessel. A PSV ratio of $\geq$2.5 has shown a good correlation with stenoses with a diameter reduction of $\geq$50% (24).

Magnetic resonance imaging (MRI)

Basic principles

Hydrogen nuclei, or protons, can be viewed as charged particles that spin around their axes. According to electromagnetic theory, this will result in a magnetic moment. When protons are placed in an external magnetic field, as in an MRI scanner, their net magnetisation vector will align with the external field, with each proton precessing around the direction of the external field. The frequency of the precession, called the Larmor frequency, will depend on the strength of the magnetic field the nuclei are exposed to. A radiofrequency wave at the Larmor frequency will tip the magnetisation vector of the protons away from the direction of the main field. The protons will thereafter realign to their equilibrium state, while at the same time emitting a radio signal, which can be detected. This, in brief, is the physical basis of the signal generation in MRI.

The rate at which this realignment occurs is defined by the T1 relaxation time, which corresponds to the time taken for the net magnetisation (in the direction of the external field) to return to 63 % of the maximum value. Concurrently with this phenomenon there is gradual dephasing of the individual magnetisation vectors of the protons, due to magnetic interactions between nearby protons. This is called called T2-relaxation, where the T2 in a tissue is defined as the time taken for the signal to decay to 37% of its original value. If the MRI sequence not compensates for spin dephasing caused by static field inhomogeneities, like in gradient echo sequences, the signal will decay according to T2*, which is shorter than T2.

The repetition time (TR) of an MRI sequence is the time between subsequent excitation radio-frequency (RF) pulses. With short TRs, protons with long T1 will not have time to regain full magnetisation. The corresponding differences in magnetisation between protons with different T1 values will translate into signal intensity differences, and the sequence will be T1-weighted. In gradient echo sequences, the flip angle is another major parameter determining the degree of T1 weighting. With large flip angles, protons with slow T1 relaxation (long T1) will regain less magnetisation than protons with short T1, resulting in T1-dependent image contrast.

The echo time (TE) of an MRI sequence is the time from the RF pulse to the detection of the signal . With a long TE, there will differences in signal contribution between from protons with different T2 relaxation times, and the sequence will be T2-weighted.

If the external magnetic field is varied in a controlled manner, by applying gradient fields, protons in different locations will be exposed to slightly different magnetic field strengths. This will lead to differences in the Larmor frequency between protons at different sites. This difference in frequency makes it possible to calculate the signal contributed by each separate volume element, in two or three directions, and hence to reconstruct an image.

K-space

The k-space is a hypothetical space consisting of different lines, which together carries all the information needed for reconstruction of the final image. Each line in the k-space corresponds to one detected RF signal, with the strength of the gradient varying for each line (phase encoding). During the signal detection, another gradient is switched on (frequency encoding). Different parts of the k-space will contribute to varying degrees to the spatial resolution and the contrast in the reconstructed image. The centre of the k-space, where the phase-encoding and frequency-encoding gradients have their lowest amplitude, is the most important part for image contrast. The periphery of the k-space, corresponding to high gradient amplitudes and thus high frequencies, contains information about image resolution. The concept of the k-space, and where in the k-space the image contrast is encoded, has important implications for the following discussion on the synchronisation between the contrast agent injection and the MRA scan.

Flow-dependent magnetic resonance angiography (MRA)

Time-of-flight (TOF)

During an MR examination, protons in stationary tissue will be exposed to repeated RF pulses, which will cause them to be saturated. This means that after an RF pulse, the protons will not have time to regain their full magnetisation before the next RF pulse is applied. Since the magnitude of the magnetisation vector at the time of the RF pulse sets a limit to the amplitude of the detected MR signal, this saturation causes a signal reduction.

Protons moving in to the imaged slice or volume will not have been exposed to previous RF pulses, and thus will have full magnetisation. This is the mechanism for the so-called inflow, or time-of-flight (TOF) effect, which causes the signal from flowing blood to be higher than the surrounding stationary tissue. This effect is exploited in TOF-MRA, which can be performed either as two-dimensional or three-dimensional acquisition. Long acquisition times and flow-related artefacts are the major disadvantages of TOF-MRA. Acquisition times of typically 5-10 min increase the risk for motion artefacts. Flow-related artifacts are of two types. Firstly, signal loss might follow from saturation of the moving protons, if the vessel is oriented in the acquisition plane or if the volume is too thick relative to the flow velocity (25). Secondly, flow turbulence, e.g. in stenotic areas, causes dephasing of the protons, and hence signal loss (25). Nowadays, TOF-MRA is mostly used for assessment of intracranial vessels.

Phase contrast (PC)

PC-MRA is another flow-dependent MRA technique. This is based on the fact that moving protons will change frequency as they move along a magnetic field gradient, resulting in a difference in phase between stationary and moving protons. By applying opposed gradients of equal size, one after the other, stationary protons will acquire no net phase shift, whereas moving protons will acquire a shift in phase that is proportional to their velocity. This phase shift is translated into signal intensity differences in the MRA image, a procedure that has to be performed in all three directions if all space components of the velocity are to be obtained. One problem arises when the velocity reaches the level corresponding to a phase shift of 180 degrees. Any further velocity increase will result in lower absolute phase shifts, a phenomenon called aliasing. In the MRA image, this will give rise to vessel areas with velocities above the threshold for aliasing to be erroneously displayed with low signal intensities, corresponding to low velocities. As a consequence, an estimation of the maximum velocity within the imaged vessel has to be made prior to any PC-MRA examination, and the aliasing limit adjusted thereafter.

In PC-MRA, artefactual flow voids may occur in regions of turbulent flow, e.g. at stenoses, which may lead to overestimation of stenoses. This is an even greater problem than in TOF-MRA, since longer echo times are used in PC-MRA in order to allow the additional gradient switching. One further disadvantage of PC-MRA is the long acquisition times, which restrict the possible scan volume and may cause artifacts from breathing, swallowing or other body movements.

Contrast-enhanced MRA (CE-MRA)

Principles

In contrast-enhanced MRA, the vessel-to-background contrast is achieved by a reduction in blood T1 induced by the injected contrast agent. With the use of a T1-weighted sequence, high signal in blood is obtained after contrast agent injection. Higher injection rates of contrast agent give higher contrast agent concentrations in blood, and hence a higher vessel signal (26).

In CE-MRA, 3D-gradient echo sequences are employed (27). Gradient sequences are used because they are faster than spin echo sequences. Furthermore, gradient echo sequences lack out-flow effects, which causes signal voids in vessels with high flow velocities in spin echo imaging. There are several reasons for choosing a 3D rather than a 2D acquisition. With a 3D acquisition there is a higher signal-to-noise ratio, since the signal from each volume element is integrated over the whole scan, as opposed to 2D imaging, where the signal acquisition is slice selective. A 3D acquisition also permits higher spatial resolution, with isotropic or near isotropic voxels, whereas in 2D-imaging the resolution in the slice selection direction is limited.

In CE-MRA, a fast sequence with heavy T1 weighting, and minimum flow-related artefacts is desirable. Hence very short TR and TE are used. The choice of flip angle is a compromise between T1 weighting (which increases with larger flip angles), and signal-to-noise ratio (SNR) (a small flip angle is necessary in order to maintain SNR if a short TR is used). The optimum flip angle depends to some degree on the concentration of the contrast agent in the blood. It has been reported, however, that similar results are obtained over a fairly large range of flip angles (28).

Flow-related artefacts are minimised in CE-MRA (28). Since the vessel signal is mainly attributed to a reduction

of blood T1 rather than to an inflow effect, saturation effects are negligible. Signal loss due to phase dispersion in areas of turbulent flow is also largely reduced compared with both TOF- and PC-MRA. This is because the vessel signal in TOF-, and PC-MRA is mainly generated during systole, when the flow velocity is highest but also when there is maximum turbulence, which causes signal loss. In CE-MRA on the other hand, the longer diastolic part of the cardiac cycle, with lower flow velocity and less turbulence, accounts for the major part of the signal. In order to further minimise signal loss from phase dispersion, the shortest echo time and smallest voxel size (with an acceptable SNR) possible should be used (27).

Further advantages of CE-MRA compared with flow-dependent techniques are shorter acquisition times, permitting breath hold and multistation examinations on modern scanners, and more efficient vessel coverage because of the freedom of choice in imaging plane orientation.

CE-MRA has displayed promising results in most body areas on evaluation (29-40), and has shown better agreement with DSA than have flow-dependent techniques in several vessel areas, e.g. the aortoiliac (30, 31) and carotid arteries (32, 33). In the coronary and cerebral arteries, however, CE-MRA has to date not proven to be as reliable as DSA, because of limits in spatial and temporal resolution (41-43).

Contrast agents for MRA

Different types of contrast agents are used in CE-MRA. These can be divided into extracellular and intravascular depending on their type of distribution after intravenous injection. All these agents affect both the T1 and T2 relaxation rates, i. e. they have both longitudinal and transverse relaxivity properties (r_1 and r_2 respectively). In order to achieve a high vessel signal, a low r_2/ r_1 is required, since the effect of a high r_1 can be counteracted by a signal loss from rapid phase dispersion if there is also a high r_2.

Extracellular contrast agents

These agents include the most commonly used contrast agents in MRI, namely gadolinium (Gd)-chelates, which show rapid leakage to the interstitium and are therefore preferentially used as first-pass agents in MRA. The Gd-chelates include gadopentetate dimeglumine (Magnevist ®, Schering AG, Germany, and Berlex, USA), gadodiamide (Omniscan ®, Nycomed Amersham Imaging A/S, Oslo, Norway), gadoteridol (ProHance ®, Bracco Diagnostics, Milan, Italy), gadoterate meglumine (Dotarem ®, Guerbet, France), gadobenate dimeglumine (MultiHance ®, Bracco Diagnostics, Milan, Italy) and gadobutrol (Gadovist ®, Schering AG, Germany). Of these, gadobenate dimeglumine differs from the other agents in two respects. It shows weak binding to plasma proteins, resulting in a higher r_1 (9.7 $mM^{-1}s^{-1}$) than with the other agents (4.3-5 $mM^{-1}s^{-1}$) (44). In addition, it is partly eliminated by hepatobiliary excretion (45). Gadobutrol is the only agent that has a concentration of 1.0 mM- all the others are 0.5 mM. The higher concentration of gadobutrol is supposed to be of benefit in CE-MRA.

Gadolinium chelates have been shown to be very safe contrast agents, without nephrotoxicity (at approved dose levels) and with a lower incidence of anaphylactoid reactions than iodinated contrast agents (46).

Intravascular contrast agents

Intravascular contrast agents (also called blood-pool agents), are confined to the intravascular space by their size. In addition, most intravascular contrast agents exhibit delayed clearance from the blood vessels, with $T_{1/2}$ in plasma in the range of hours. This property may be of advantage in MRA since it allows prolonged scan times. This can be utilised either for improvements in SNR by the acquisition of multiple NEXs, or for imaging of several vascular territories on one occasion. The main disadvantage of steady-state MRA with intravascular contrast agents is the coexistent signal in veins, which may obscure the arteries.

Different types of intravascular contrast agents are being tested in clinical trials. These include macromolecular Gd chelates such as MS-325 (Schering AG, Germany) and iron oxide based agents (ultrasmall iron oxide particles, USPIO) such as NC100150 Injection (Clariscan ®, Nycomed Amersham Imaging A/S, Oslo, Norway) and SHU-555 C (Schering AG, Germany). In addition to having an intravascular distribution, both types have markedly increased relaxivities compared with the extracellular agents (47).

Superparamagnetic iron oxides (SPIOs) are very efficient T2* relaxing agents, and are eliminated from the blood by uptake in the reticulo-endothelial system. These properties have made them suitable for use as negative contrast agents for imaging of the liver, spleen and lymph nodes (48-54). SPIOs also have T1-reducing properties (55), which however for large size SPIOs are counterbalanced by the large T2 relaxivity. With smaller size SPIOs, the r_2/ r_1 quotient is reduced, primarily by a reduced r_2, but to some extent also by an increase in r_1. With a size less than 50 nm (ultrasmall superparamagnetic iron oxides, USPIOs), the r_2/ r_1 is reduced to a level that these agents can be utilised as positive T1-contrast agents for vascular enhancement (56-61).

Timing strategies

Several techniques may be employed in order to synchronise the contrast medium injection with the MRA scan. The simplest is the "best guess" method, where the contrast delay is estimated on the basis of known clinical parameters such as age, weight, cardiac status etc. This, however, is also the most unreliable method, because of the large interindividiual variations in contrast circulation time (62, 63).

In the test bolus technique (62, 63) , a small bolus of contrast agent (typically 2 ml) is injected at the same rate as in the imaging scan, and flushed with saline, whereafter repeated slices are obtained at a position in the beginning of the vascular territory of interest. From this scan, the arrival time of the contrast bolus can be estimated, either by visual inspection of the slices or from signal intensity versus time curves. One drawback of this technique is that the test bolus injection will cause enhancement of the urinary bladder and in the background tissues, e.g. in the renal parenchyma. Furthermore, the test bolus scan takes some extra time. For these reasons triggered techniques have been developed.

These can be divided into automatic and fluoroscopic types. In the automatically triggered sequence (64), a slice including the vessel of interest is repeatedly scanned after injection of the whole contrast agent volume. The signal intensity in an operator-defined voxel is continuously measured, and the imaging scan is started when a certain threshold level is reached. In the fluoroscopically triggered technique (65), the contrast arrival is monitored in real-time, by acquiring a repeatedly updated slice including the vessel to be studied. When the contrast arrival is detected, the operator manually switches to the imaging scan. Both these techniques are commonly combined with a centric k-space acquisition, in order to synchronise the centre of the k-space with the peak arterial concentration of the contrast agent (65).

In the last few years fast sequences have permitted dynamic acquisitions, whereby multiple phases of the scan are acquired after injection of the contrast agent (66). The phase with the maximum arterial signal is then chosen retrospectively for evaluation. One disadvantage of this approach is an inevitable reduction in spatial resolution compared with a longer scan, and another is that the data sets will be very large.

Iliac arteries

Haemodynamically significant stenoses of the iliac arteries are a common cause of intermittent claudication (67). Accurate grading of such stenoses is of major importance for decisions regarding surgical or endovascular intervention. The identification and treatment of ipsilateral iliac stenoses also have a large impact on the long-term patency after more distal reconstructive procedures.

For assessment of the iliac arteries, DSA has been used, preferably in combination with intra-arterial pressure measurements. Duplex scanning has emerged as a non-invasive alternative (24, 68). It has the disadvantage of having at least some degree of operator dependence, and that the measurements are sometimes difficult in obese patients or on account of obscuring bowel gases. Contrast-enhanced MRA has also shown good correlation with DSA (30, 31, 38, 40) and has yielded superior results compared with TOF-MRA for grading of iliac artery stenoses (30, 31). To our knowledge, however, there have been no previous studies in which CE-MRA has been compared with intra-arterial pressure measurements, which are accepted as a more clinically relevant reference method.

Since atherosclerotic lesions tend to be present in multiple locations (1), there is most often a need for an evaluation not only of the aortoiliac arteries but also of the renal arteries and outflow vessels. This has been possible in recent years with MRA by the implementation of fast, breath hold, sequences for assessment of the renal arteries (38), and multistation sequences for complete evaluation of the arterial tree from the aorta to the feet (69-71).

Investigated topics

The main limitation of CE-MRA compared with DSA is a lower spatial and temporal resolution. For this reason CE-MRA has not been fully accepted for the assessment of small-calibre vessels such as branches of the cerebral arteries (41), or the coronary arteries(42) , for which respiratory and cardiac motion is also a problem. Another limitation is occasional poor visualisation of vessels, due to improper timing of scanning in relation to contrast agent injection.

There are different ways for reducing these limitations. Steady-state imaging, preferably with intravascular contrast agents, makes it possible to increase the spatial resolution. More efficient T1-reducing contrast agents may improve the visualisation of small-calibre vessels, and may also yield a higher spatial resolution with preserved SNR. Improved reliability of vessel visualisation can also be achieved with improvements in the timing of scanning versus contrast agent injection.

The lower spatial resolution of CE-MRA compared with that of DSA may at least partly be counterbalanced

by the advantage of MRA in being a 3D examination. The proper choice of image display technique must be made, however, since the accuracy of a CE-MRA examination is dependent on what evaluation method is used (72, 73). In steady-state imaging, the major issue is how to selectively visualise the arterial tree.

In studies presented in this thesis, different aspects of CE-MRA were investigated. A comparison was made between CE-MRA, DSA and DUS using intra-arterial pressure measurements as reference (paper I), where different image display methods (MIP and MPR) were also compared. The consequence of a delayed contrast bolus arrival at the distal parts of the aortoiliac vessel was analysed, and a novel timing technique was assessed (paper II). New high relaxivity T1 contrast agents were evaluated for use in CE-MRA, both for first-pass (paper III) and steady-state imaging (paper IV).

AIMS OF THE STUDY

General aim

To evaluate the use of contrast-enhanced MRA with different contrast agents and imaging strategies

Specific aims

To compare CE-MRA with DSA and DUS regarding the detection of haemodynamically significant iliac artery stenoses, with pressure measurements as reference method

To assess the difference between proximal and distal contrast bolus arrival time in CE-MRA of the iliac arteries

To determine whether the distal signal in iliac artery CE-MRA is preserved to a larger extent with the use of a modified test bolus scheme than with a fluoroscopically triggered sequence using centric view order

To establish the least efficient dose of gadobenate dimeglumine for CE-MRA of the iliac arteries

To determine whether CE-MRA of the iliac arteries, using gadobenate dimeglumine, increases the diagnostic quality compared with TOF-MRA

To assess the usefulness of the blood-pool agent NC100150 Injection for enhancement of the large abdominal vessels

To assess the dose and echo time dependency of the vascular signal with the blood-pool agent NC100150 Injection

TECHNIQUES

MRA

All MRA examinations were performed at 1.5 T, except in study IV, where examinations were performed at both 0.5 T and 1.5 T. A body coil was used in all studies. The gradient strength was 10 mT/m at the time when studies I and IV were conducted, but had been upgraded to 23 mT/m prior to studies II and III. In study III, some examinations were performed at other centres, with different scanners, all operating at 1.5 T. In all CE-MRA studies, a 3D RFspoiled GRE sequence was used. In study III, a 2D TOF-MRA technique was also used. The sequence parameters used in the studies are given in Table 1.

The contrast agents used for the CE-MRA examinations were gadodiamide (Omniscan ®, papers I-II), gadobenate dimeglumine (MultiHance ®, paper III) and NC100150 Injection (Clariscan ®, paper IV). In order to synchronise the scan with the contrast injection, a test bolus examination was performed in studies I-III. A fluoroscopically triggered sequence was also evaluated in study II. No timing techniques were used for the steady-state acquisitions (paper IV). A power injector was used for all contrast agent injections except for the injections of NC100150 Injection in study IV. The contrast agent injections were followed by injections of saline (20 ml) at the same rate as the contrast agent injections (papers I-III).

DSA and IAPM (Paper I)

The common femoral artery was catheterised on the symptomatic side, using the Seldinger technique (74). A 6F introducer was inserted, through which a 5F endhole catheter was placed with its tip in the lower aorta. Images of the lower aorta and iliac arteries were obtained in the frontal view and in right and left 20^0 oblique views.

Simultaneous pressure recordings were obtained from the 5F catheter and the 6F introducer. If the aortofemoral pressure gradient was less than 20 mm Hg, the measurement was repeated after injection of 60 mg papaverine into the lower abdominal aorta through the 5F catheter.

DUS (Paper I)

An Acuson XP 128 apparatus (Acuson, Mountainview, Ca, USA) was used, equipped with a 5 MHz transducer. In the iliac arteries, a PSV ratio of 2.5 was used as the threshold for a stenosis with a diameter reduction of ≥50%. Occlusions were diagnosed when no flow was detected.

Investigated vessel (paper nr)	TR (ms)	TE (ms)	Flip angle (^{0})	FOV (mm)	Matrix	Slice width (mm)	Scan time (s)	Contrast volume (ml)	Injection rate (ml/s)
Iliac arteries (I)	12-16	5-5.7	50	360	261 X 512	4	61-90	30 (n=8) or 40 (n=22)	1
Iliac arteries (II), Dual-station	4.2	1.2	40	400	256 X 195	3.9	20	30-44	2
Iliac arteries (II), BolusTrak	4.2	1.2	40	400	256 X 195	3.9	20	40	2
Iliac arteries (III), CE-MRA	<7	<2.8	40	360-400	Voxel size : 2x2x2	2	19-26	0.025-0.4 ml/kg	2
Iliac arteries (III), TOF-MRA	Not spec.	Not spec.	Not spec.	360	Not spec.	3	600	NA	NA

A

TR (ms)	TE (ms)	Bandwidth (Hz/pixel)	Matrix (freq.x phase)	Echo type	Half scan (%)	Field strength (T)
8.2	3.0	748	256X164	PARTIAL	50	0.5
12	4.8	221	256X196	FULL	60	0.5
16	8	145	256X196	FULL	60	0.5
20	12	145	256X179	FULL	55	0.5
8.3	2.9	748	256X164	PARTIAL	50	1.5
9.9	3.9	434	256X164	FULL	50	1.5
14	8	434	256X164	FULL	50	1.5
18	12	434	256X164	FULL	50	1.5

B

Table 1.
MRA sequence parameters for studies I-III (a) and IV (b).

MATERIALS, METHODS AND RESULTS

MRA, DSA, and DUS compared with IAPM *(*Paper I*)*

Material

CE-MRA and DSA of the iliac arteries were performed in 30 patients, in whom DUS had shown iliac stenoses or inconclusive results. Intra-arterial pressure measurements were made in 25/30 patients (27 aortoiliac arteries).

Methods

The arterial tree was divided into the lower aorta, common iliac arteries and external iliac arteries, resulting in five segments per patient. Each segment was graded according to the most severe stenosis, on a three-grade scale: 0=0-49% diameter reduction, 1=50-99% reduction and 2=occlusion. The MRA and DSA examinations were evaluated by two different observers, each blinded to the result of the other modality. Two MRA evaluations were performed, either with the use of MIPs only (MRA-MIP), or with the use of source images and also curved multiplanar reformatations (MPRs) (MRA-MPR).

	Sensitivity(%)	Specificity(%)	Positive predictive value (%)	Negative predictive value (%)
MRA-MIP	81[64-98]	75[45-100]	89[76-100]	60[30-90]
MRA-MPR	76[58-94]	75[45-100]	89[74-100]	55[25-84]
DSA	86[71-100]	88[65-100]	95[85-100]	70[42-98]
Duplex	72[47-90]	88[47-100]	93[66-100]	58[28-85]

Table 2.
Sensitivity, specificity, positive predictive value, and negative predictive value [95% confidence interval] for MRA, DSA, and Duplex regarding significant iliac artery stenoses, with pressure gradients as reference.

	Sens. (%)	Spec. (%)	PPV (%)	NPV (%)	*k*
MRA-MIP	91[82-99]	79[71-87]	66[54-78]	95[91-100]	0,67[0,50-0,85]
MRA-MPR	81[69-92]	89[83-95]	76[63-88]	92[86-97]	0,72[0,52-0,92]
Duplex	63[48-79]	85[78-92]	63[48-79]	85[78-92]	0,43[0,21-0,64]

Table 3.
Sensitivity (Sens.), specificity (Spec.), positive predictive value (PPV), negative predictive value (NPV), and weighted kappa *value (k), with 95% confidence intervals for MRA, and Duplex regarding significant aortoiliac artery stenoses, with DSA as reference.*

A pressure gradient of 20 mm Hg or more, with or without peripheral vasodilatation, was considered a positive finding for a haemodynamically significant stenosis. In addition, cases where pressure measurements were not possible because of occlusions were also categorised as haemodynamically significant lesions.

In order to calculate the sensitivity and specificity of the different modalities, a dichotomous classification was used. Negative findings consisted of vessels that were normal or mildly stenosed. Vessels with severe stenoses (50-99% diameter reduction) or occlusions were classified as positive findings. The statistical significance of differences in sensitivity and specificity was tested with a logistic regression model predicting the diagnostic outcome from the patient identity, vessel segment and method chosen, in the appropriate subpopulation. These calculations were carried out in JMP 3.1 (SAS Institute, Inc., Cary, NC, USA). A p value of 0.05 was chosen as the threshold for statistical significance.

Pressure gradient measurements were performed in 25 patients, bilaterally in two cases. The measurements were regarded as inconclusive in two patients, in one patient because the distal pressure recording was considered irrelevant as the distal measurement was made from within a tight stenosis, and in the other because measurements after papaverine injection showed higher pressures distal to a stenosis, which was believed to be a result of diminishing vasodilatation. In addition to the 25 conclusive pressure gradient measurements, there were four cases in which an occlusion in the common or external artery was found during ipsilateral catheterisation. This was considered to be equivalent to the finding of a haemodynamically significant pressure gradient, and these cases were added to the group of segments with pressure gradient measurements, resulting in 29 aortoiliac segments. Assessable MRA and DSA results were obtained on all 29 sides with conclusive pressure measurements. Conclusive DUS results were obtained on 27/29 sides.

Results

Pressure drops of ≥20 mm Hg or occlusions verified by catheterisation were found in 21/29 arteries (72%). The sensitivity, specificity, and positive and negative predictive values of the methods, with pressure measurements as the reference method, are listed in Table 2. DSA had the highest values for all these parameters (along with DUS for specificity). There were no statistically significant differences between the methods regarding the detection of lesions of proven haemodynamic significance ($p>0.05$).

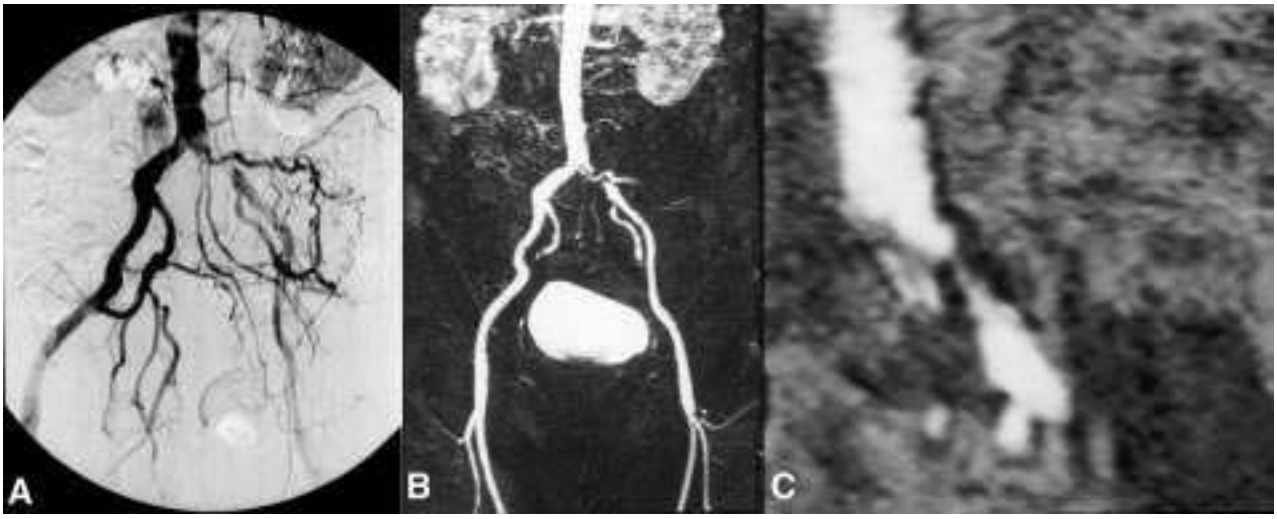

Figure 1.
A left-sided common iliac artery is seen to be occluded on a) DSA and b) maximum intensity projection of MRA. A curved multiplanar reformat of the MRA c) shows a severely stenosed, but patent vessel.

In 30 patients, conclusive DSA investigations were made in 148/150 vessel segments. One DSA examination covered only one side of the iliac territory, resulting in three examined segments. There were assessable results in 145/148 vessel segments with MRA-MIP and in 140/148 vessel segments with MRA-MPR. Three external iliac arteries were excluded for the following reasons: vessel partially outside the field of view (FOV) (1), signal loss due to ipsilateral metal hip replacement (1), and signal loss due to vascular stents (1). The MRA-MPR evaluation could not be made in one patient because of lost raw data. The corresponding number of vessel segments for DUS was 132/148. There were inconclusive scans in two aortas and four iliac segments. In five cases unilateral Duplex ultrasound scanning of the iliac artery was performed.

The gradings of each segment with MRA and DUS compared with DSA are shown in Table 3. Both MRA methods had a higher sensitivity than DUS for the detection of lesions with a diameter reduction of at least 50 %, and these differences were statistically significant. The sensitivity differed non-significantly between the MRA methods (p=0.23), whereas the specificity was higher with MRA-MPR than with MRA-MIP, and this difference was marginally significant (p=0.053). The agreement between methods according to the 3-grade scale was evaluated with the weighted kappa coefficient ($_W$) (75). The calculated coefficients indicated a higher correlation between the MRA evaluations and DSA than between DUS and DSA (Tab. 3).

MRA-MPR compared favourably to MRA-MIP concerning the assessment of vessel patency (Fig. 1). MRA-MIP showed occlusions in five segments where patent vessels were seen with DSA, while with MRA-MPR there was only one segment that was falsely graded as occluded. Six segments were graded as occluded with DUS where DSA showed no occlusion.

Timing techniques (Paper II)

Material

CE-MRA of the iliac arteries was performed in 27 patients with clinically suspected haemodynamically significant stenoses. Two different timing strategies were applied. A modified (dual-station) test bolus technique was used in 14 patients, and a fluoroscopically triggered technique (BolusTrak ®) was used in 13 patients.

Methods and results

In the dual-station test bolus group, a test bolus of 2 ml was injected in one second. In the test bolus scan, two axial slices were dynamically acquired; one in the superior part of the abdominal aorta, and the other at the level of the common femoral arteries. The contrast delay time to both the aorta and the common femoral artery (symptomatic side or bilaterally) was determined. The contrast delay time to the common femoral artery was used as the scan delay in the imaging scan (when both femoral arteries were measured, the longest delay was chosen). The difference in contrast delay time between the aorta and the femoral artery was used to determine the duration of the contrast injection. The injection time was lengthened with this difference, from a baseline of 15 s (30 ml at 2 ml/s), with a constant injection rate. This was done in order to ensure that the bolus was long enough to cover both the proximal and distal vascular parts during central k-space acquisition.

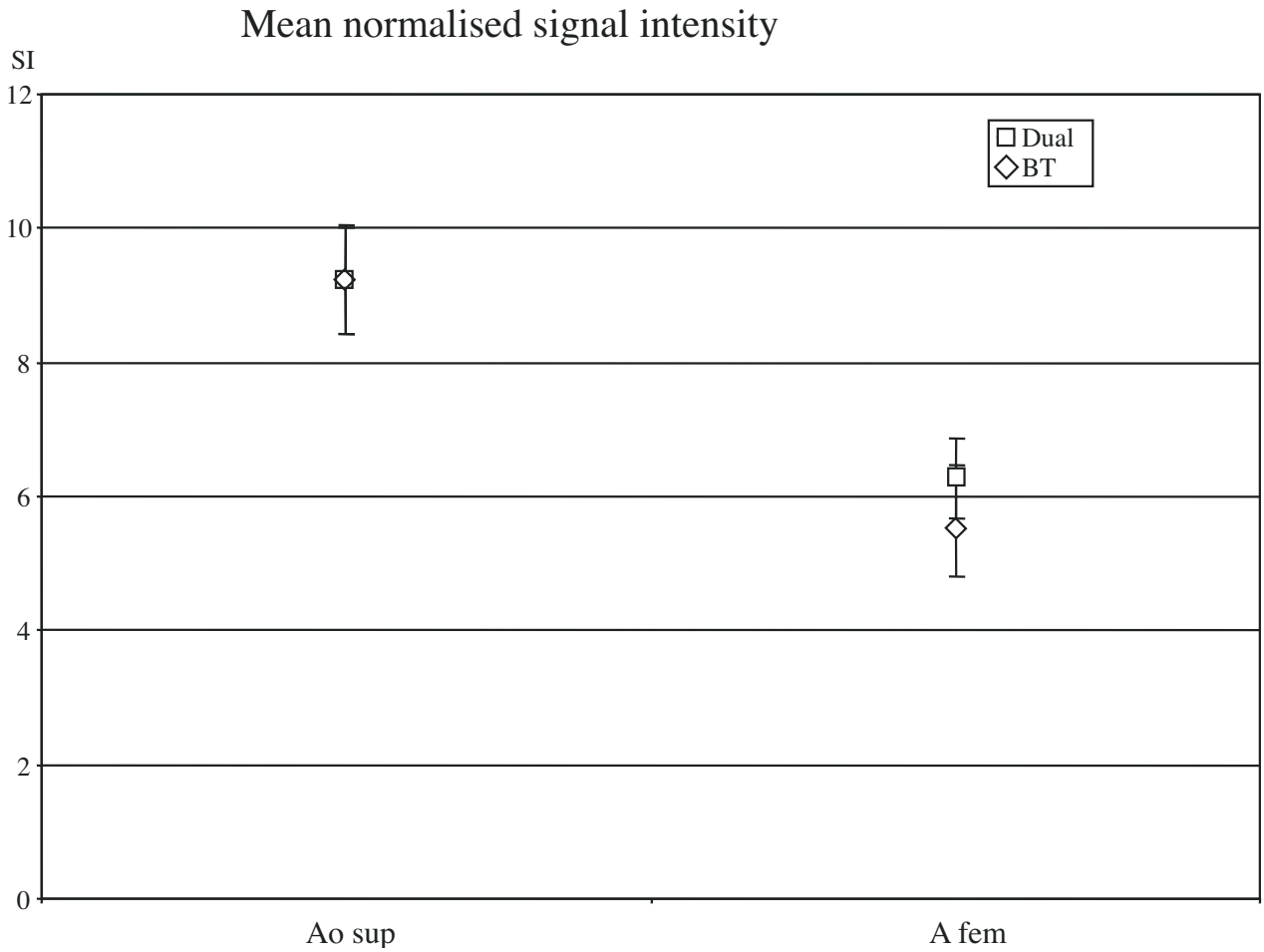

Figure 2.
Mean signal intensities normalised to fat, with 95% confidence intervals, for the superior part of the abdominal aorta and femoral artery (on the side with lowest signal). Lower SI is seen distally with both techniques, but no significant differences are seen between the two timing techniques.

In the second group the contrast arrival time was monitored fluoroscopically and the 3D-GRE scan was initiated when contrast was seen in the proximal abdominal aorta (BolusTrak ®, Philips Medical Systems, Best, The Netherlands). Centric k-space acquisition was used in this sequence. The contrast agent was injected at a rate of 2 ml/s to a total volume of 40 ml. This scan was then repeated after a delay of about 45 s. Measurements and stenosis gradings were performed on the first scan.

Measurements of signal intensity (SI) were carried out in six locations in each scan: the superior part of the abdominal aorta, aortic bifurcation, junction of common and external iliac artery (bilaterally), and common femoral artery (bilaterally). If an occlusion was found at a site of measurement, that site was discarded from the analysis. The signal intensity from subcutaneous fat was measured in four locations (superior and inferior parts on each side) in the middle slice of the imaging volume. The mean of these ($SI_{Fat\ mean}$) was used for calculating the normalised SI (SI_N), where $SI_N = SI / SI_{Fat\ mean}$. In this way scaling differences were taken into account.

The mean normalised SI for the aorta and femoral artery is shown for both timing techniques in Figure 2. SI was significantly lower distally than proximally ($p<0.001$ for both techniques). Similar SIs were seen in the aorta, whereas a tendency to a higher mean signal in the femoral artery was noted with the dual-station technique compared with the BolusTrak method. No statistically significant differences were observed between the two techniques, however ($p=0.99$ for the aorta and $p=0.211$ for the femoral artery). The levels of significance were calculated with Student's two-tailed t-test, assuming normally distributed variables and equal variances.

In each patient, the mean of the signal intensities in the six locations with the standard deviation and coefficient of variation (CV) was calculated. CV was used for

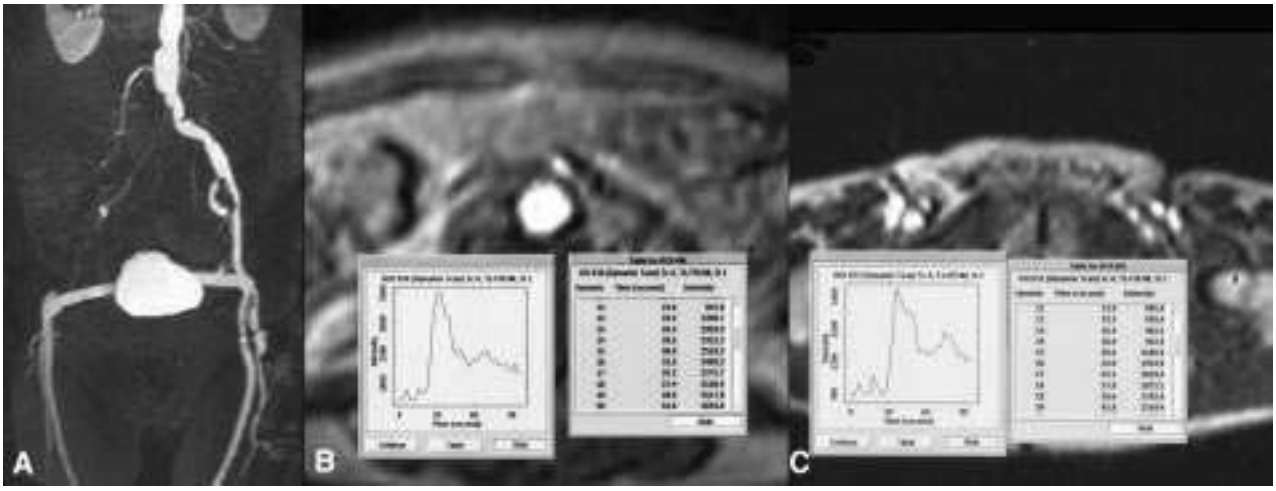

Figure 3.
A case with a right-sided iliac artery occlusion, and a cross-over graft, examined with the dual-station technique (a). In (b), the signal intensity versus time curve obtained at the test bolus scan is shown for the aortic measurement. The corresponding curve obtained at the right femoral artery is shown in (c). A difference in peak signal intensity of 6.6 s is calculated between the two sites. Despite the large difference in bolus arrival time, the outflow vessels are well delineated on both sides.

comparing the degree of signal homogeneity between the methods. Student´s two-tailed t-test (76) was again used for assessment of the level of significance of differences between the dual-station test bolus technique and the BolusTrak method. A marginally significant (p=0.10) difference was observed, with a higher mean CV with the BolusTrak method (0.20) than with the dual-station technique (0.15).

In the group with both proximal and distal measurements of the bolus transit time, we found aorto-femoral differences in contrast bolus arrival time of 0-7 s. The mean difference was 3.0 s, corresponding to a mean contrast volume of 36 ml in the dual-station group. In 3/14 patients (21%) the difference was more than 5 s.

The vessels were divided into five segments: aorta, right and left common iliac artery, and right and left external iliac artery. Each segment was graded according to the most severe stenosis: 0= 0=49% diameter reduction, 1= 50-99% diameter reduction and 2= occlusion. Occlusions were seen in six iliac arteries in the dual-station group and in two iliac arteries in the BolusTrak group. The vessels distal to the occlusions were visualised in all cases with the dual-station method (Fig. 3). In one patient examined with the BolusTrak technique, there was no detectable vascular signal distal to an iliac occlusion, the length of which was confirmed by a later scan (Fig. 4). In another patient in the BolusTrak group, the femoral artery was not visualised on one side on the first scan but was seen to be patent on the later scan. In this case there was a high-grade stenosis proximal to the non-visualised vessel.

Gadobenate dimeglumine-enhanced MRA compared with TOF-MRA (Paper III)

Material

At nine different centres, 136 patients in whom iliac artery stenoses were suspected on clinical grounds or with any modality were examined. All patients underwent first unenhanced (2D TOF-MRA), and then contrast-enhanced MRA (Table 1). On-, and off-site evaluations were available in 135 and 134 of these patients, respectively.

The study plan was approved by the local ethics committee at each centre and written informed consent was obtained from each patient before inclusion.

Methods and results

The patients were randomised to one of four dose groups, 0.025, 0.05, 0.1, and 0.2 mmol/kg body weight (bw). Because of a systematical dosing error mainly at one centre, five different doses were actually administered (0.0125, 0.025, 0.05, 0.1 and 0.2 mmol/kg bw).

The vessels were divided into nine segments: I = distal 2 cm of the abdominal aorta, II = proximal 1 cm of the common iliac artery, including the ostium (right and left), III = main part of the common iliac artery (right and left), IV = iliac bifurcation including the proximal 2 cm of the internal iliac artery (right and left) and V = external iliac artery (right and left). Each segment was evaluated

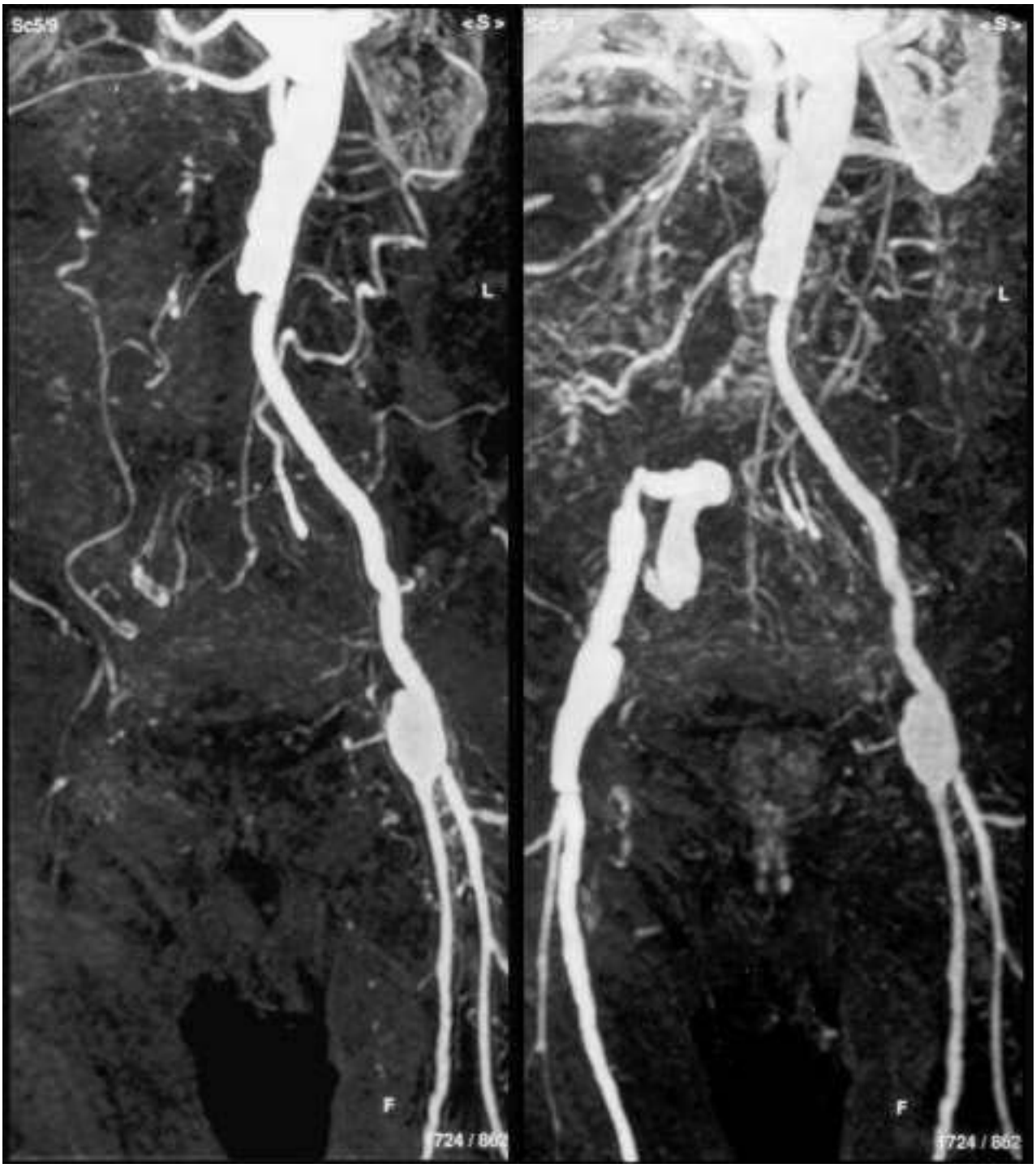

Figure 4.
Example of a non-visualised distal vessel segment in a patient examined with the BolusTrak technique. There is a right-sided occlusion of the common iliac artery, from the aortic bifurcation to the origin of the internal iliac artery. In the fluoroscopically triggered scan (a), the refilled external iliac artery distal to the occlusion is not visualised, but is clearly demonstrated on the delayed scan (b).

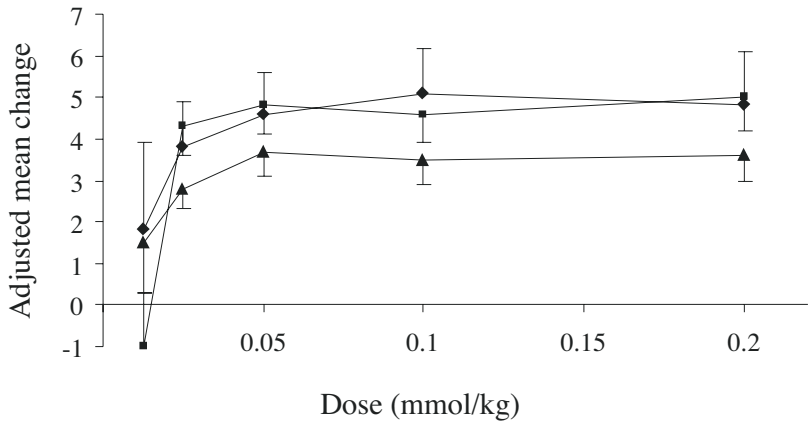

Figure 5.
Adjusted mean change (+95% confidence interval) in total diagnostic quality score from pre-contrast to post-contrast. Diamonds = off-site reviewer 1; Squares = off-site reviewer 2; Triangles = on-site reviewers.

regarding the diagnostic quality, number of lesions detected, confidence in lesion characterisation, and ability to grade stenoses. Two off-site reviewers, blinded to the type of MRA technique and the dose level, made these assessments. In addition to the off-site assessments, an on-site assessment of the diagnostic quality was made by one investigator for each study site. This investigator was blinded to the dose level for the CE-MRA examinations, but not to the type of MRA technique.

The primary efficacy end-point in the present study was the change in the total diagnostic quality score from baseline in each patient. A three-grade scale for diagnostic quality was used: 0=impossible to detect or exclude lesions, 1=moderate diagnostic information, and 2=adequate diagnostic information, lesions can definitely be detected or excluded. The total diagnostic quality score for each examination was calculated as the sum of the scores for each segment. The five actual doses of gadobenate dimeglumine were compared using analysis of covariance with the total baseline (TOF-MRA) score as covariate. Adjusted means (including 95% confidence

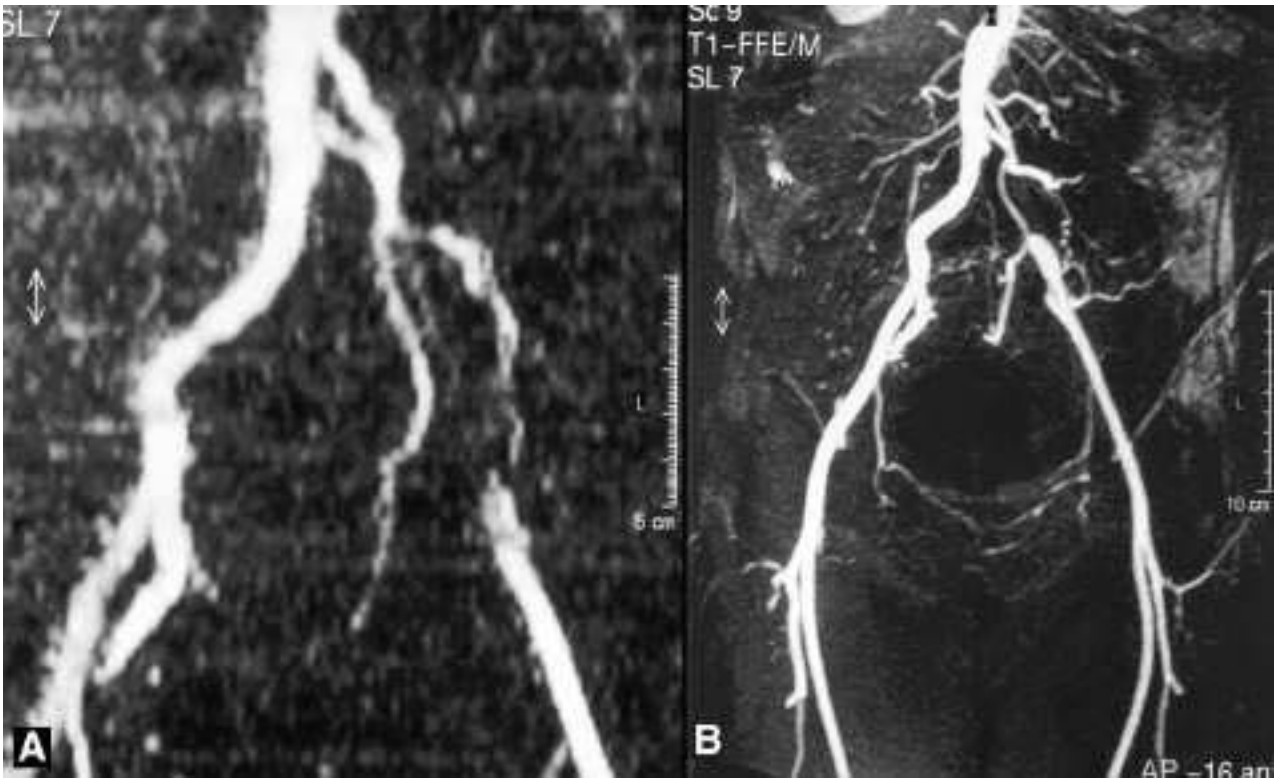

Figure 6.
TOF (a), and CE-MRA (0.2 mmol/kg bw gadobenate dimeglumine) (b) image in patient with occlusion of the left common iliac artery. Note the signal void in the proximal part of the left external iliac artery on the TOF image. In the CE-MRA study there is also better depiction of small-caliber vessels (lumbar arteries and collaterals).

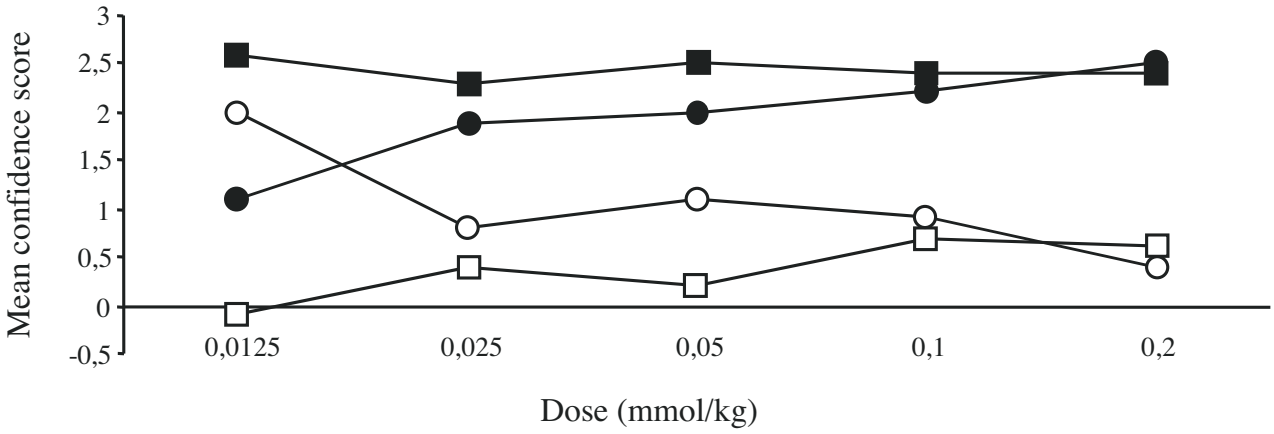

Figure 7.
Mean pre- and post-contrast confidence scores.
Open squares: pre-contrast, reviewer 1;
Closed squares: post-contrast, reviewer 1.
Open circles: pre-contrast, reviewer 2;
Closed circles: post-contrast, reviewer 2

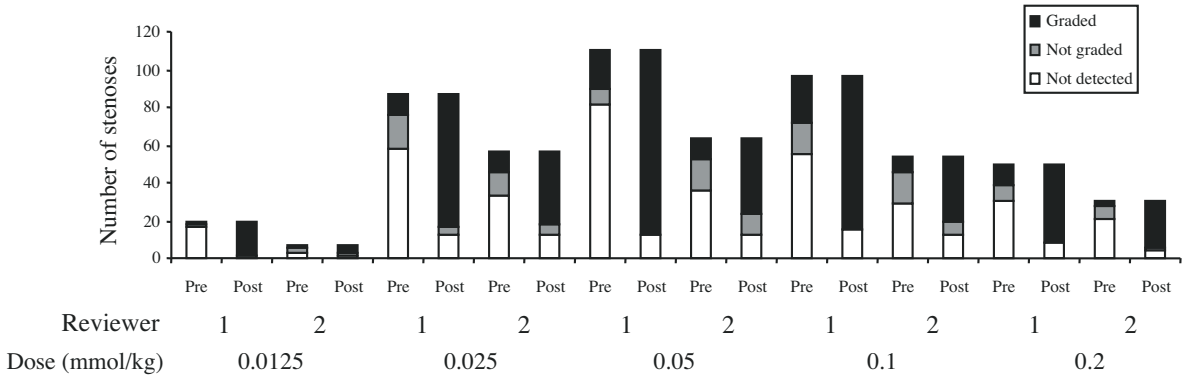

Figure 8.
Visualisation of stenoses pre-and post-contrast.

intervals) and p values from the F test for overall effect were calculated. The dose-response curve was plotted using the mean response at each dose.

As shown in Figure 5, the mean diagnostic quality score was significantly higher in the contrast-enhanced examinations than in the TOF examinations at all doses of gadobenate dimeglumine above 0.0125 mmol/kg bw. An example of the benefit of CE-MRA compared with TOF-MRA is shown in Figure 6. There was an increasing trend with dose in terms of diagnostic quality, with plateaus at 0.1 mmol/kg (off-site reviewer 1) and at 0.05 mmol/kg (off-site reviewer 2). The overall dose effect on diagnostic quality was marginally significant for off-site reviewer 1 ($p=0.064$) and highly significant for reviewer 2 ($p<0.001$). A highly significant over-all dose effect was also seen for the on-site reviewers ($p=0.005$). No clear dose-related trends were observed for the other parameters.

The total number of lesions was calculated for each examination. In the majority of patients there was an increase in number of lesions per patient in the contrast-enhanced examinations except the 0.0125 mmol/kg bw group for reviewer 2. The number of patients with any lesions detected also increased in all groups except in the group with 0.0125 mmol/kg bw for reviewer 2.

A four-grade scale for confidence in lesion characterisation was used, with 0=doubtful, 1=possible, 2=likely and 3=certain. The mean confidence in lesion characterisation increased in the majority of patients except in the 0.0125 mmol/kg bw dose group for reviewer 2 (Fig. 7).

Regarding lesions characterised as stenoses, the possibility of grading these accurately was assessed as either 0=not possible or 1=possible. The proportion of stenoses that were visualised clearly enough for reliable grading was higher at the CE-MRA examinations than at the TOF-MRA examinations in all dose groups for both reviewers (Fig 8).

Physical examination, recording of vital signs, electrocardiographs, and laboratory evaluation of blood and urine samples were performed in each patient. Monitoring for adverse events was carried out at fixed time points up to 24 h after injection of the contrast agent. There were no serious adverse events that were considered to be possibly related to the contrast agent. All 15 events with an unknown, possible or probable relationship with the contrast agent were of mild or moderate intensity. The incidence rates of adverse events with a presumed causal relationship to the contrast agent were 0/10 (0%), 2/33(6.1%), 3/34 (8.8%), 2/34 (5.9%) and 3/25 (12.0%) in the 0.0125, 0.025, 0.05, 0.1, and 0.2 mmol/kg dose groups respectively. There were no overall trends in vital signs or ECG that were considered to be clinically significant. In two patients, changes in laboratory parameters were considered as adverse events (proteinuria, haematuria, decreased red blood cell count and decreased albumin in one patient, and increased creatinine and decreased white blood cell count in another patient). All these events were mild in intensity, and self-resolving.

Abdominal vessel enhancement with NC100150 Injection (Paper IV)

Material

The study population consisted of 18 healthy male volunteers. The subjects were divided by dose and field strength into six groups (3 subjects in each), given 1.0, 2.5 or 4.0 mg Fe/kg bw respectively and examined at 0.5 or 1.5 T. Two subjects in the 4.0 mg/kg bw group at 0.5 T were not examined because of technical problems with the scanner. The study plan was approved by the local ethics committee and written informed consent was obtained from each subject before inclusion.

Methods and results

NC 100150 (30 mg Fe/ml) was given into the antecubital vein at a rate of 1-3 ml/s. The imaging sequences took place 5-15 min after the contrast medium injections. Four breath hold sequences with different parameters were accomplished for each subject (Table 1).

SI measurements were made on the manoeuvring console. For each subject and sequence, a slice near the middle of the aorta and inferior vena cava (IVC) was chosen. Regions of interest (ROIs) were drawn in the aorta, IVC, the vessel background, noise outside the subject and in a marker with T1=172 ms, T2=143 ms (field- and temperature-independent in the relevant range), placed at the side of the subject´s abdomen. The minimum pixel count for the ROIs was 35. ROIs in the vessels were placed centrally, excluding the proximity of the vessel wall. The mean SIs for the regions were recorded.

The signal intensities were normalised to those of the marker. Since the sequences with different echo times differed slightly in their TR values, we chose to rescale the intensities to the same (=the longest) TR for each field. It was then possible to make some estimation of T2* values for different doses. Blood samples were obtained from the subjects 5 min post injection. The T1 values were measured in an NMR analyser (PC120 Bruker Minispec) operating at 0.47 T, using an inversion recovery pulse sequence with at least 10 different recovery times. The T1 values at 1.5 T were calculated. We adopted the standard spoiled FLASH signal expression (77) and with known T1 and T2 values of the marker and T1 values from the blood the measured signal intensities were rescaled to the same TR. Normalised and rescaled signal intensities are denoted SI´. Contrast to noise (C/N) ratios were calculated for the vessels ($C/N=(SI_{vessel}-SI_{surrounding})/SD_{noise}$).

The mean SI´ for the aorta and IVC with the different doses and echo times at 0.5 and 1.5 T are shown in Figure 9. With the shortest echo time SI´ showed a positive dose response at both field strengths. This is exemplified in Figure 10. Increasing the echo time caused a progressve decrease in SI´ in both vessels at all three doses (Fig. 9). This effect was more pronounced with higher doses.

The C/N ratios for the shortest echo times at the two field strengths are shown in Figure 11. Higher values were seen at 1.5 T than at 0.5 T over the whole dose range.

The quality of aortic delineation was judged by one of two reviewers after initial consensus training. This evaluation was not blinded for sequence parameters or dose level. The examinations were divided into very unsatisfactory (score=0), unsatisfactory (score=1), satisfactory (score=2) or very satisfactory (score=3). The mean scores for aortic delineation were highest with 2.5-4 mg Fe/kg bw at both field strengths (Fig. 12). Higher scores for aortic delineation were assigned at 1.5 T .

The mean SI´ was higher from the IVC than from the aorta for all doses and echo times at both field strengths (Fig. 10). The C/N ratios were also higher for the IVC than for the aorta (Fig. 11). R2* estimations are shown in Figure 13. At the higher field strength the calculated R2* was higher in the aorta than in the IVC. A general observation was an inhomogeneity of the vessel signal, most notably in the aorta, with stripes of higher signal along the walls.

Artefacts were noted and allocated to one of the following categories: loss of signal, focal signal increase, blurring of border, or other. The impact of artifacts on the

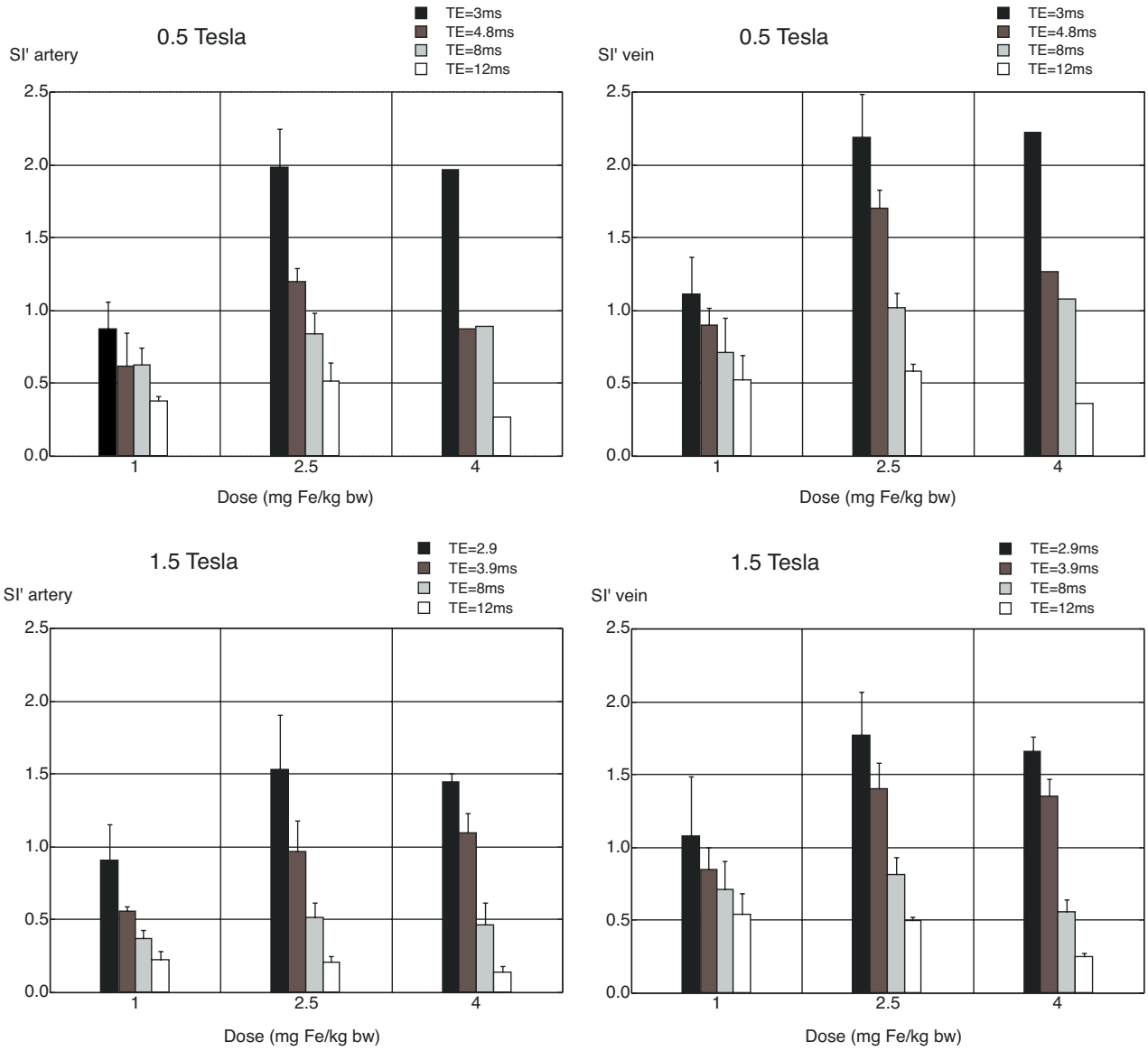

Figure 9 (a-d).
Rescaled and normalised signal intensity (SI´) in the aorta and the IVC with different doses and echo times at 0.5 and 1.5 T.

image quality was assessed, and graded as: not seriously affected/no impact, image quality seriously affected or images not diagnostic. Artefacts were noted in 10/48 sequences (focal signal increase in four, blurring of borders in three, loss of signal in two and not categorised in one). Eight of 10 sequences with artifacts were performed at 1.5 T. The image quality was judged not to be seriously affected in any of the cases.

Recording of vital signs, physical examinations, ECG and withdrawal of blood samples were carried out pre- and post-injection at fixed time points in order to monitor for adverse events. No serious adverse events were observed.

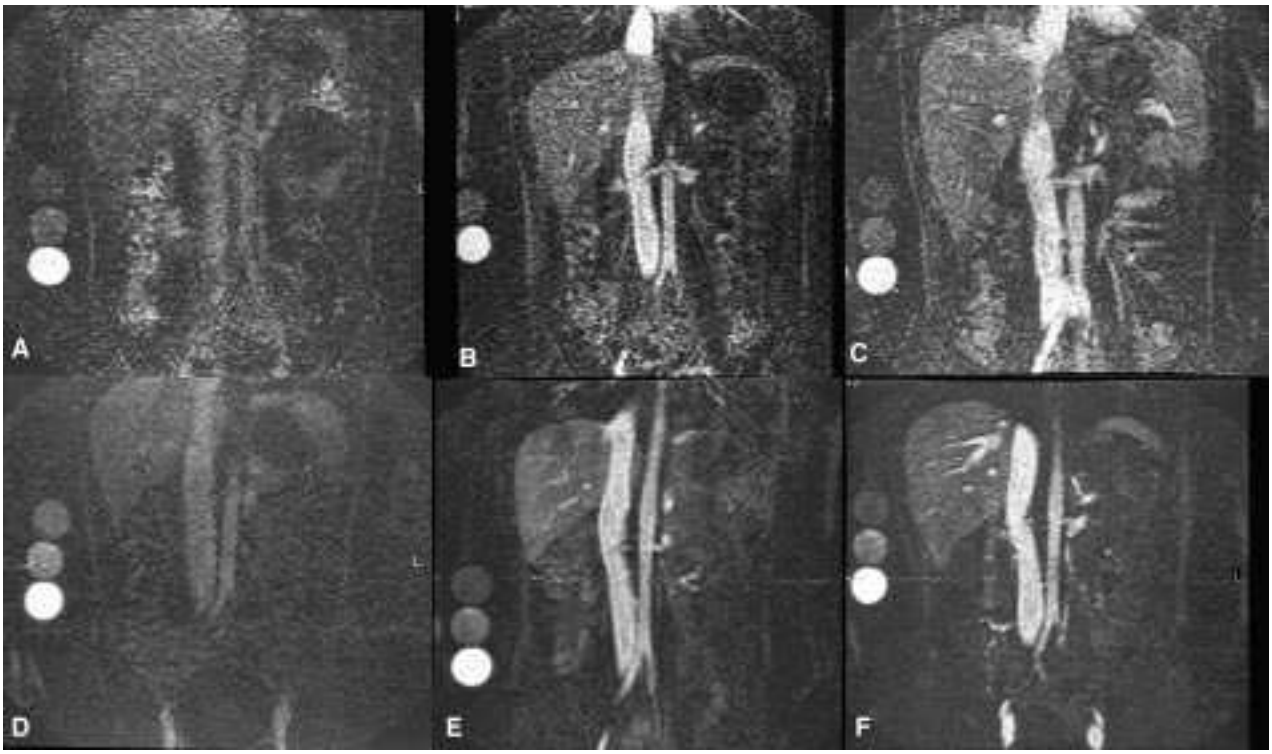

Figure 10.
Example illustrating the dose dependence at both field strengths with the shortest echo time. Figure a-c shows images of the aorta and the IVC at 0.5 T from three subjects who were injected with a) 1.0 mg Fe/kg bw, b) 2.5 mg Fe/kg bw and c) 4.0 mg Fe/kg bw. Figure d-f shows the corresponding comparison at 1.5 T, d) 1.0 mg Fe/kg bw, e) 2.5 mg Fe/kg bw, and f) 4.0 mg Fe/kg bw. At both field strengths higher signal intensities are seen with the two higher dose levels. Image noise is increased at the lower field strength. At the right side of the abdomen are seen three markers with known T1 and T2 values.

DISCUSSION

In the studies described in this thesis, a number of parameters influencing the diagnostic quality of a CE-MRA examination were investigated. The biodistribution and relaxivity of the contrast agent determines the possible T1 reduction that can be obtained (papers III and IV). In first-pass imaging, proper synchronisation of the scan to the contrast injection is of crucial importance (paper II). The diagnostic accuracy is also influenced by the way the acquired data set is evaluated. Maximum intensity projections, multiplanar reformatations, and source images were compared in study I.

Comparisons with DSA, pressure measurements, duplex (paper I), and TOF-MRA (paper III) were made.

Comparisons with other techniques

CE-MRA, DUS and DSA compared with IAPM (Paper I)

In study I we investigated iliac artery MRA compared with DSA and duplex ultrasound scanning, with pressure gradient measurements as reference method. We found no statistically significant differences between MRA, DSA and DUS concerning the detection of haemodynamically significant iliac artery stenoses (Tab. 2). The rationale for the use of pressure gradient measurements as reference method rather than DSA was that the pressure (and hence flow) distal to a stenosis is largely preserved until a certain critical degree of stenosis is reached (3). With a further increase in vascular narrowing, a profound decrease in blood pressure and flow is seen. Small variations in the degree of stenosis can thus imply large differences in flow reduction. Furthermore, the critical level of vascular narrowing is dependent on the calibre of the vessel, as well as on the volume flow rate (11). Tandem lesions of subcritical degree may also cause significant pressure drops (78). These factors explain why morphological methods have shortcomings concerning the assessment of borderline and tandem stenoses. In addition, it may be unfair to evaluate a 3D method against a 2D reference method.

Different absolute or relative values for mean or systolic pressure gradients, with or without pharmacological vasodilatation, have been proposed as thresholds for a haemodynamically significant iliac artery stenosis. In line with a previous report(12), we chose to use a

systolic pressure gradient of 20 mm Hg after peripheral vasodilatation with papaverine to represent the lower limit for a significant stenosis. Some technical aspects are important for obtaining valid pressure recordings. The proximal and distal pressure recordings should preferably be obtained simultaneously. Otherwise the pressure gradient will be affected by normal fluctuations in the pressure level, and be more uncertain. This is especially important after peripheral vasodilatation, when larger temporal pressure variations occur. Simultaneous pressure recordings can be obtained in two ways. Catheters can be placed from both sides, one ipsilateral to the measured side into the femoral artery, and one from the contralateral side into the lower aorta. This method has the disadvantage of requiring bilateral groin punctures. The coaxial system that we used requires only unilateral puncture. The drawback of this technique, however, is that the inner catheter has to be placed across the pressure-measured segment, which might introduce an artifactual pressure gradient, depending both on the vessel calibre and on the catheter dimension (14, 79-81). Given the normal size of the iliac arteries, and the diameter (1.6 mm) of the catheter employed, the recorded pressures were probably not significantly altered. Care must be taken not to make the pressure recording within a narrowed segment, where the measurement may be influenced by a local flow disturbance.

Discrepancies between pressure measurements and the findings in morphological studies can occur in low-flow situations. Since the pressure drop is proportional to the blood flow velocity (3), a lesion that is apparently significant on DSA or MRA might not cause a significant pressure drop if the peripheral resistance is high or the cardiac output is low.

Using this technique for pressure gradient measurement, it was not possible to locate a detected significant lesion within the iliac artery. For this purpose, a pull-back technique (14) may instead be performed.

The results of this study show that intraarterial pressure measurements remain an important tool for the identification of haemodynamically significant stenoses. Neither of the tested methods could accurately identify or deny the presence of haemodynamically significant stenoses in all proven cases. This is logical, since both MRA and DSA are morphological methods, and the significance of a stenosis is also related to flow, as stated above. Duplex has the ability to provide information on flow velocities, and volume flow, but with the PSV ratio used in this study, it is actually also a morphological method, since the quotient between PSVs in neighbouring vessel segments only depends on the vessel diameters. Attempts have been made to estimate the pressure gradient using duplex velocity data and a simplified Bernoulli equation, with varying degrees of success (82). Similar trials have been made with MRI, using a phase contrast technique, to obtain information on flow velocities (83). Schoenberg et al tried a different approach in the renal arteries, using phase contrast MRI. They found that flow velocity profiles obtained on each side of a stenosis to be useful for the assessment of the haemodynamic significance(84). This approach could possibly be implemented in the iliac arteries, and eliminate the need for invasive pressure measurements.

CE-MRA and DUS compared with DSA (Paper I)

In order to compare our results of study I with those of previous studies, we not only made comparisons with pressure measurements as reference method, but also compared MRA and DUS with DSA as reference (Tab. 3). With regard to the detection of stenoses with a diameter reduction of 50% or more, we found sensitivities for MRA of 81% (MIP) and 76% (MPR), and a specificity of 75% (both MRA techniques). Somewhat higher sensitivities (93-100%) and specificities (89-100% in three studies, and 62-87 % for two observers in one study) have been reported for MRA in previous studies(30, 31, 38, 40). Two of these (38, 40) were conducted with higher performance gradients, which permitted the use of shorter echo times and injection rates, because of the shorter acquisition times. This would lead to an increase in SNR, which at least partly may explain the better results.

Regardless of which evaluation method was chosen, MRA showed a significantly higher sensitivity than duplex scanning for the detection of relevant stenoses, with DSA as reference method. In our series, the sensitivity and specificity of duplex scanning for detection of $\geq$50% stensosis were 63% and 85%, respectively. Higher values for sensitivity and specificity have been reported with duplex in previous studies. Currie et al reported a sensitivity of 91% and a specificity of 93 % (68). All their examinations were performed by the same investigator, and the examination time was reported to be 60-90 minutes. In our study, the duplex examinations were carried out by different investigators, in a routine clinical setting, with less time per patient (typically 20-30 minutes). We regard the discrepant results as an illustration of the high operator dependence of duplex ultrasound scanning.

CE-MRA compared with TOF-MRA (Paper III)

In study III we found a significantly higher diagnostic quality with CE-MRA (using gadobenate dimeglumine)

of the pelvic arteries compared with TOF-MRA. This gain was observed at dose levels as low as 0.025 mmol/kg. Further evidence of the improved diagnostic accuracy achievable with gadobenate dimeglumine-enhanced MRA compared with TOF-MRA is provided by the results for lesion detection, confidence in lesion characterisation, and ability to grade stenoses.

Regarding the increased numbers of lesions detected with CE-MRA, the absence of a recognised reference method such as digital subtraction angiography (DSA) means that different interpretations are possible. However, the assumption that the present findings are a true indication of increased diagnostic accuracy is supported by previous studies in which CE-MRA has proven considerably more reliable than unenhanced MRA for the detection and grading of stenosis (30-33). It is likely that the improvement seen on gadobenate dimeglumine-enhanced images compared with unenhanced images is a reflection of the well-known limitations of TOF-MRA, such as artefactual signal loss from in-plane saturation or spin dephasing in areas of turbulent flow. The use of CE-MRA instead of TOF-MRA may have clinical consequences, by for instance more adequately showing the length of occlusions (Fig. 6).

The superiority of CE-MRA over TOF-MRA has also been shown in previous studies of the iliac arteries. Poon et al (31) compared stenosis gradings of the iliac arteries using CE-MRA, cardiac gated TOF-MRA, and conventional (x-ray) angiography. Significant differences in gradings were observed between TOF-MRA and x-ray angiography, but not between CE-MRA and x-ray angiography. Snidow et al (30) found improved accuracy regarding stenosis grading in the common and external iliac arteries with CE-MRA compared with TOF-MRA; this was statistically significant for one observer ($p=0.046$) and marginally significant for the other observer ($p=0.095$).

Contrast-enhanced MRA also has advantages over flow-dependent MRA for assessment of the neck vessels. The free choice of imaging plane permits coverage of both the anterior and posterior supra-aortic vessels, from the arch origins to the circle of Willis. This allows detection of tandem lesions (e.g. in the arch origins or in the carotid siphon). Flow-related artifacts from turbulent flow or in-plane saturation are also virtually eliminated, as also are artifacts from swallowing and motion, as a result of the shorter scan duration. Previous studies on carotid artery MRA have indeed shown improved accuracy in the grading of carotid artery stenoses with use of contrast-enhanced MRA compared with flow-dependent techniques (32, 33).

Timing strategies (Paper II)

Accurate timing of the MRA scan in relation to the arrival of the contrast bolus at the vascular region of interest is crucial for obtaining high quality angiograms (85, 86). In study II we found that the contrast arrival time varied markedly in different parts of the aortoiliac territory. To the best of our knowledge, this aspect has not been investigated before in MRA. We tried a dual-station test bolus examination in order to take this variation into account. Compared with the BolusTrak method, we did not find any significant improvement in normalised distal signal, although a marginally significant improvement in vascular signal homogeneity was observed. We consider this to imply that the delay between detection of the contrast bolus and the start of scan is sufficient in most patients for adequate contrast filling in the distal vessels. The importance of a varying contrast arrival time is illustrated, however, by the two failures in the BolusTrak group. In one of three cases with occlusions, inaccurate timing caused non-visualisation of the vessel distal to the occlusion. In the dual-station group, on the other hand, the vessels distal to occlusions were visualised in all six cases. The other case in the BolusTrak group had a high-grade stenosis proximal to the non-visualised vessel.

Other strategies may be used in order to visualise vessel segments with varying contrast arrival times. With modern scanners, fast sequences permit dynamic acquisitions, ensuring an adequate contrast concentration in a certain vessel segment in at least one of the acquisitions (66, 87). This is accomplished, however, at the expense of a decrease in spatial resolution. Another way would be to use a very long injection time, and time the scan so that the contrast agent would definitely have arrived at the distal part of the vascular territory. This would necessitate a decrease in the contrast agent injection rate and hence a reduced SNR. Using a fluoroscopically or automatically triggered timing technique, one could start the scan when the bolus has arrived at the distal parts, but then the bolus would have passed the proximal part at the time of central k-space acquisition in cases with large differences in contrast arrival time. With the dual-station technique, this difference is recognised, and the injection time can be adjusted accordingly.

The superior reliability of the dual-station method for visualisation of the distal signal follows from a more accurate synchronisation between the scanning of the central k-space and the bolus passage through the distal vascular territory. Even with the dual-station timing technique, however, there was some loss of signal along the vessel path (Fig. 2), which is probably inevitable in view of the progressive dilution of the contrast agent.

Inflow effects may also contribute to a higher proximal SI.

Apart from a reduction in flow velocity distal to a significant stenosis (3), other factors may contribute to slow passage of a contrast agent bolus. Both a reduced cardiac output and ectatic vessels would have this effect.

Another consequence of improper timing of scanning versus contrast injection is the occurrence of artefacts related to rapid variation of the contrast medium concentration during acquisition of central parts of the k-space. Such artefacts have been demonstrated both theoretically and experimentally (85, 86). They may decrease the diagnostic accuracy, but can be avoided if the contrast agent injection is properly synchronised with the scan.

The feasibility of our proposed timing technique is shown by the fact that measurements of bolus arrival were possible in the femoral arteries in all cases, despite the small vessel calibre. A problem could arise in cases with occlusions in the measurement region. In such cases a repeated test bolus scan with a coronal slice orientation could be used, which might increase the possibility of detecting the bolus arrival somewhere in the volume.

Some methodological aspects of this study are worth mentioning. Since the T1 shortening in the blood is proportional to the contrast agent injection rate, we used a constant injection rate. The minimum contrast volume was 30 ml with the modified timing technique, which was lower than with the BolusTrak techniques (40 ml). With the modified technique, the contrast agent volume was increased in proportion to the difference in proximal and distal contrast arrival times. The rationale for using a lower minimum volume with the dual-station technique was that we did not want the mean delivered volume with this technique to exceed the volumes used with the BolusTrak method. An overall increase in contrast agent volume would make the comparisons between the timing techniques difficult, since it has been shown that an increase in contrast agent volume in itself (with constant injection rate) causes an increase in the peak concentration of the contrast agent bolus (88, 89).

All scans were made with breath hold. Using the BolusTrak technique, this called for an instruction to the patient at the time of contrast arrival, before the start of the scan. This introduced at least some degree of operator dependence as regards the timing of the scan.

In order to obtain slices from two levels, the slice updating frequency of the test bolus scan was reduced by half, resulting in one slice/1.4 s for each station. If a higher frequency is required, two separate test bolus scans at different levels could be performed instead.

A more reliable comparison would have been possible if both techniques had been used in each patient. This was not possible, at least not in one session, as the contrast dose would then have exceeded the approved limit.

In conclusion, we found in some cases large differences in contrast arrival time between proximal and distal parts of the aortoiliac territory. This can lead to a poor vessel signal or even non-visualisation of distal vessel parts. Our results stress the importance of taking not only the proximal, but also the distal contrast arrival time into consideration. A timing technique adjusting for any difference in arrival time was proposed, and found to be feasible. This phenomenon is expected to increase in importance with the continuing evolution towards shorter scan times, since a certain time difference between proximal and distal parts will then correspond to a larger shift in k-space.

Contrast agents

Conventional extracellular gadolinium chelates (Papers I-II)

In studies I and II, the gadolinium chelate gadodiamide (Omniscan ®) was used in the CE-MRA sequences. In these studies no comparisons were made with unenhanced MRA sequences or other contrast agents. No dose evaluations were made.

The biodistribution and relaxivity properties of gadodiamide are similar to those of the other available non-specific, extracellularly distributed gadolinium chelates, and no clear advantages of one contrast agent over the others have been demonstrated in clinical practice (44, 90).

Gadobenate dimeglumine (Paper III)

In a phase II MRA study on the contrast agent gadobenate dimeglumine, the total diagnostic quality score showed an increasing trend with increasing dose up to a dose of 0.05-0.1 mmol/kg body weight, after which there was an apparent plateau up to a dose of 0.2 mmol/kg body weight. It is likely that these findings are a true reflection of the clinical efficacy of gadobenate dimeglumine, i.e. that doses higher than 0.1 mmol/kg body weight provide little additional diagnostic information over and above that obtained with a dose of 0.1 mmol/kg, but it should be borne in mind that the primary endpoint of the present study was a subjective diagnostic quality score as opposed to a score based on signal intensity measurements. This

choice was made under the assumption that "diagnostic quality" is a clinically more relevant parameter than signal intensity, since the clinical objective is to acquire images with adequate information for the detection or exclusion of relevant pathology rather than images with the maximum achievable vessel signal. Previous studies have shown that vessel signal intensity increases whith increasing dose of gadobenate dimeglumine in a dose-dependent manner up to a dose of 0.2 mmol/kg gadobenate dimeglumine irrespective of the rate of administration (91).

A further possible, though less likely explanation for the plateau observed above a dose of 0.1 mmol/kg body weight is the appearance of T2* effects at the higher doses. Such an effect would tend to decrease the signal and thus counter the T1 effect observed at the lower doses. Such T2* effects, however, have not previously been seen in studies on gadobenate dimeglumine in MR angiography. Moreover, the possibility cannot be excluded that the observed plateau at the highest dose levels is due to an increased frequency of artefacts at these doses. The results concerning technical adequacy, however, reveal no evidence of a dose-related increase in artefact frequency.

An obvious limitation of the present study is that no active comparator was used. The reason for this is that when the study was initiated, no gadolinium-based contrast agent was approved for MR angiography. Although no conclusions can be drawn from this study on the comparative efficacy of gadobenate dimeglumine relative to other gadolinium agents, previous studies in which gadobenate dimeglumine was compared with gadopentetate dimeglumine for MRA of the abdominal aorta showed that the former agent produced a higher vascular peak enhancement (29% on average) of longer duration than the latter agent at the same dose and flow rate (92). The absence of any formal correlation with DSA was due partly to the fact that the primary aim of the study was to establish the most suitable dose for MRA of the pelvic arteries. In addition, the subjects of the present study comprised patients with suspected pathology in the region of the pelvic arteries rather than patients with a high chance of serious disease, for which DSA is normally indicated. It should also be noted that with the limited number of projections available with DSA, this technique is not necessarily the ideal reference standard. In many cases MRA may display a stenosis better than DSA (93).

A further drawback of the study design was that different volumes of contrast agent were used in the different dose groups (between 0.025 ml/kg for the 0.0125 mmol/kg group and 0.4 ml/kg for the 0.2 mmol/kg dose group). With the injection rate kept constant, variation of the contrast agent volume might lead to differences in the fraction of the k-space sampled with an adequate blood contrast agent concentration. This might be considered an issue of concern, since the vascular signal in CE-MRA is dependent on an adequate blood contrast concentration during acquisition of central parts of the k-space. With the lowest dose a volume of just 0.025 ml/kg was injected. For a 70 kg person this implies a total volume of 1.75 ml, injected over a period of just 0.875 s. Although bolus lengthening during the passage through the lungs is likely to occur, this injection regimen might still result in an insufficient duration of blood T1 shortening. In the present study this might imply that the results for the lower doses were worse than might otherwise have been expected if the contrast bolus volume had been kept constant through the dose range.

This study has shown that gadobenate dimeglumine is a well tolerated contrast agent for MR angiography of the pelvic arteries and that a dose of 0.1 mmol/kg body weight is appropriate for most examinations. Previous studies have established improved T1 relaxivity and vascular enhancement characteristics of gadobenate dimeglumine compared to conventional, extracellularly distributed gadolinium contrast agents deriving from a decreased tumbling rate of the gadobenate molecules in vivo due to weak and transient interactions with serum

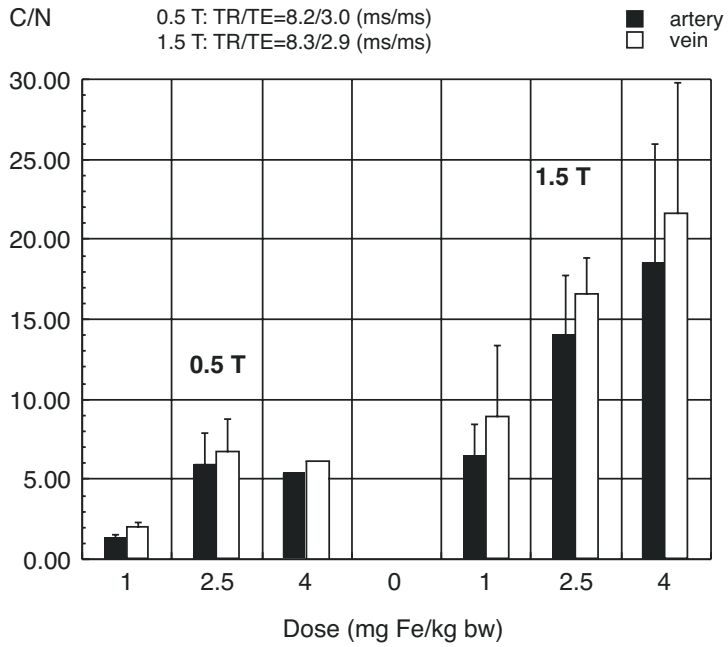

Figure 11.
Contrast to noise (C/N) ratios for the aorta and the IVC with the shortest echo time and different doses at both field strengths. There seems to be a positive dose response for C/N at 1.5 T. At 0.5 T, only one subject in the high dose group was examined.

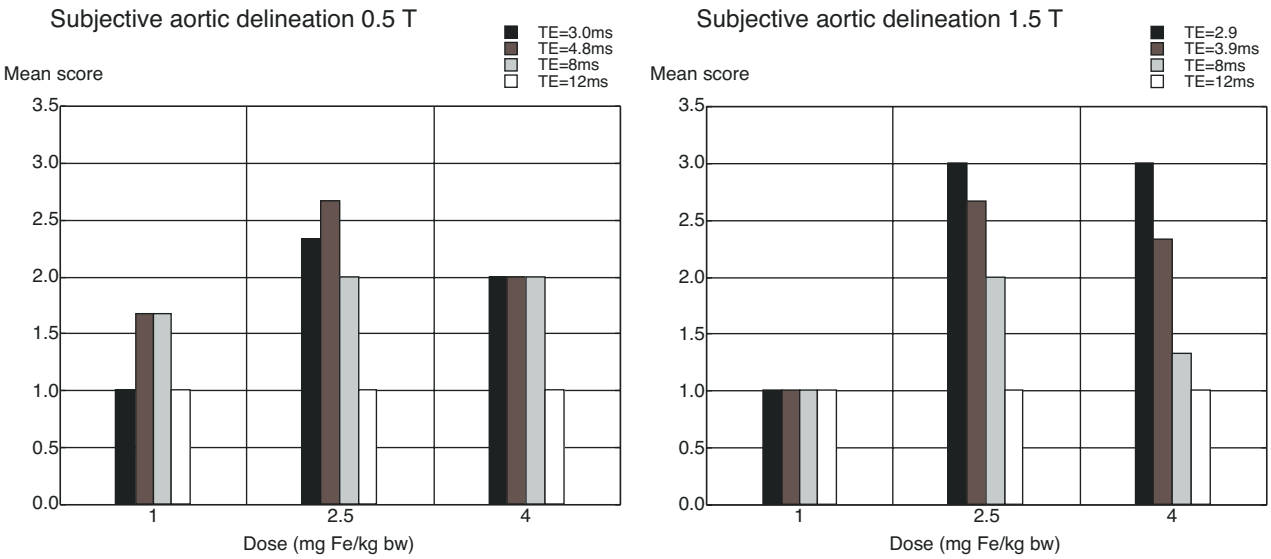

Figure 12.
Scores for aortic delineation at a) 0.5 T and b) 1.5 T with different doses and echo times.

albumin (92, 94). It remains to be determined whether the capacity of gadobenate dimeglumine for weak protein interaction offers similar advantages over the recently developed intravascular contrast agents (59, 95, 96), regarding which venous signal enhancement is a principal point of concern.

NC100150 Injection (Paper IV)

In study IV we found that the USPIO blood-pool agent NC100150 Injection (Clariscan ®) was an efficient and safe agent for vascular enhancement. At the shortest echo time and 1.5 T, CNR showed a positive dose response in both the aorta and the IVC over the whole dose range. At 0.5 T the results were equivalent for 2.5 and 4.0 mg Fe/kg bw. The results for 4 mg Fe/kg bw at the lower field strength are uncertain, however, since only one subject was examined in that group. The vascular signal was strongly dependent on the echo time, and this was accentuated with increasing dose. This is attributed to the high r_2 of USPIOs.

It is likely that T2* effects will dominate at the high blood concentrations that are obtained when high injection rates are used, and first-pass MRA with NC100150 Injection may thus be a challenge. The T2/T2* effects may on the other hand be utilised for perfusion imaging (95).

We found lower SIs in the centre of the vessels, most notably in the aorta, and overall lower SIs in the aorta than in the IVC. This is most likely a result of some signal loss from pulsatile flow, which is more pronounced in the arteries. Flow compensation was not used, as we wanted to be able to use as short an echo time as possible. A more pronounced enhancement of the veins than of the arteries was also found in a previous study on another USPIO blood pool agent (60).

The difference in R2* between the aorta and the IVC at 1.5 T, but not at 0.5 T, must be explained in another way. The difference in haemoglobin oxygenation level between arteries and veins might give rise to (field dependent) differences in susceptibility that could explain this difference. The results of recent in vitro comparisons of different doses of NC100150 Injection in whole blood do indeed support the idea that T2* effects with the use of NC100150 Injection are dependent on the oxygenation level (97). Minimum T2* effects were observed at an oxygenation level and contrast agent concentration at which intra- and extracellular magnetisation levels were equal. The difference in R2* between the aorta and IVC thus seems to be an effect of different degrees of susceptibility matching between the intra- and extracellular compartments.

The increase both in CNR and in the subjective quality of delineation at 1.5 T compared with 0.5 T is as expected, since SNR increases with increasing field strength.

The sequences with varying echo times differed somewhat with regard to other parameters also. The reason for using different repetition times (and hence the need for rescaling the SIs) was that we wanted the TR to be as short as possible at each echo time, so that the scan could be performed within one breath hold. An alternative way would have been to acquire a multi-echo

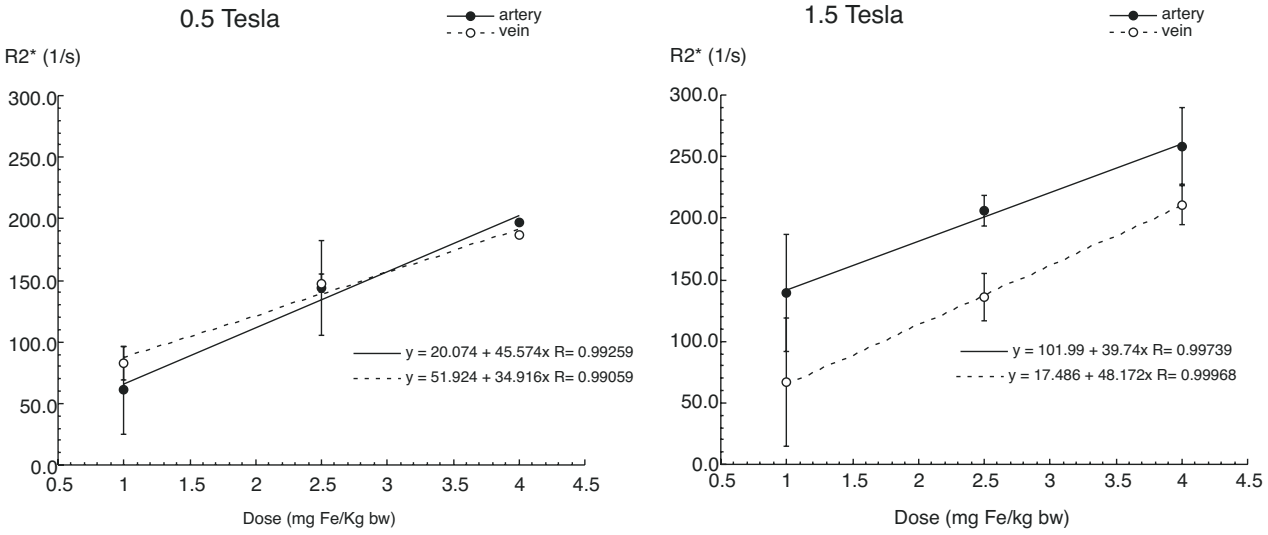

Figure 13.
Calculated R2 at a) 0.5T and b) 1.5 T for the aorta and the IVC. Increase in dose results in higher R2*, with similar slope of the curves for the different vessels at both field strengths. Note the difference in R2* between the two vessels at 1.5 T.*

sequence. The use of a partial echo as well as a wider bandwidth at the shortest echo time was a consequence of the wish to minimise the echo time.

In conclusion, these preliminary results indicate that NC100150 Injection is an efficient and well tolerated agent for steady-state vascular enhancement. The results are in good agreement with those of another study, in which NC100150 Injection was assessed for enhancement of the pulmonary arteries (98). The importance of a short echo time is stressed. A dose of 4.0 mg Fe/kg bw is recommended at 1.5 T. The observed difference in signal intensity (both field strengths) and R2* (1.5 T) between the aorta and the IVC may be utilised for discrimination between arteries and veins.

Image post-processing (Paper I)

The three-dimensional nature of the CE-MRA examination is a definite advantage over a two-dimensional modality such as DSA.The use of DSA as a reference method, even only for morphological evaluations, may be questioned. In a recent study on carotid artery stenoses, using 3D-rotational angiography as reference method, 3D-TOF-MRA showed higher accuracy for stenosis grading than DSA (93). In another comparison of CE-MRA and DSA, in a study with in vitro assessments of carotid endarterectomy specimens as reference method, CE-MRA showed better performance than DSA (99).

The three-dimensional data set acquired in MRA can be displayed in different ways. The most common method for demonstration is maximum intensity projections, whereby the object is displayed in freely chosen projections, at an arbitrary number of angles. In each projection, only the volume element with the highest signal intensity in a certain direction is displayed (100). It has been shown that stenoses may be overestimated when evaluated with MIPs alone (72). It is recommended that source images also be analysed when stenoses are being graded (27). Additional information may be obtained from multiplanar reformatations, by which slices at any desired orientation in the three dimensions can be obtained. This makes it possible to measure diameters and areas perpendicular to the vessel axis, regardless of the vessel orientation. If a very tortuous vessel is to be analysed, so called curved MPRs can be calculated. In a curved MPR, the vessel is displayed as if it were confined to the displayed plane, so that the whole course can be assessed simultaneously.

In study I, with pressure measurements as reference method, we did not find any statistically significant differences in performance between MRA using MIPs only and MRA with the additional use of source images and multiplanar reconstructions. Source images and multiplanar reconstructions were valuable, however, for discrimination between tight stenoses and occlusions. With DSA as reference method, MRA-MPR showed a marginally significantly higher specificity than MRA-MIP.

The volume rendering technique (VRT) is a post-processing method that uses the entire image data set, as opposed to MIP (and also SSD), which only uses part of the acquired data (22). VRT has been increasingly used in CT angiography, where it has shown higher accuracy than the other techniques (101, 102), but little in MRA, because of the lack of a universally comparable signal

intensity scale. With contemporary state-of-the art computers, VRT image parameters can be adjusted in real-time (101, 102), which may permit successful incorporation of VRT into MRA.

In steady-state MRA, overlying veins are a major problem in assessments of possible arterial lesions. Different strategies have been suggested to overcome this difficulty. Wang et al used the difference in oxygenation level between arteries and veins to distinguish between them (103). This was done by using the higher susceptibility of the deoxyhaemoglobin in veins to cause a phase shift compared with that in the arteries. One disadvantage of this technique is that it only works for vessels that are aligned with the main magnetic field. Another way of eliminating the veins is the so called seeding technique, whereby the operator places a marker in the structure to be eliminated, after which the computer recognises adjoining structures and automatically eliminates them (104). The volume rendering technique might prove useful also in this context also. Using VRT, overlying veins could interactively be assigned a high transparency value in order not to obscure arterial lesions.

Future prospects

A further increase in the diagnostic accuracy of CE-MRA is expected as a result of improvements in both hardware (by stronger gradients and dedicated coils with improved sensitivity) and software (faster sequences) and more efficient contrast agents. This is likely to lead to the replacement of invasive procedures by CE-MRA in further vascular territories, such as the cerebral and possibly the coronary arteries, where limits in speed and spatial resolution have restricted its usefulness (41-43). Compared with conventional x-ray angiography, MRI also has the advantage of being able to acquire physiological information, such as perfusion and diffusion data (25), and also of permitting tissue characterisation, e.g. of carotid artery plaques (105).The trend towards increasing use of CE-MRA will probably also be reinforced by an increasing awareness among referring physicians and patients of MRA as a non-ionising, reliable alternative to conventional angiography.

Furthermore, atherosclerosis is recognised as a generalised disease (1, 2), and the ability of MRA to assess large and, if necessary, multiple vascular territories may in future prove beneficial for screening and monitoring of drug therapy.

CONCLUSIONS

CE-MRA is a reliable alternative to DSA for detection of haemodynamically significant iliac artery stenoses.

In CE-MRA of the iliac arteries, the use of MPRs and source images is of value for differentiation between high-grade stenoses and occlusions.

Differences in contrast bolus arrival time between the aorta and femoral artery may be large enough to result in non-visualisation of distal vessels when a fluoroscopically triggered centric view order CE-MRA sequence is used.

A dual-station timing technique for CE-MRA of the iliac arteries, taking delayed contrast bolus arrival times in distal vessels into account, was found feasible, and resulted in higher signal homogeneity compared with the fluoroscopically triggered sequence.

CE-MRA of the iliac arteries using gadobenate dimeglumine results in improved diagnostic quality compared with 2D-TOF-MRA at doses from 0.025 mmol/kg bw.

CE-MRA of the iliac arteries showed a positive dose response with gadobenate dimeglumine up to a dose of 0.05-0.1 mmol/kg bw.

Using the USPIO blood pool agent NC100150 Injection for enhancement of the abdominal vessels, a positive dose response was found at short echo times at both 0.5 T and 1.5 T.

The echo time dependence of vascular signal intensity with NC100150 Injection increased with increasing doses.

A difference in estimated R2* between the aorta and the IVC was found when using NC100150 Injection.

ACKNOWLEDGEMENTS

I wish to express my sincere gratitude to all those who have, in different ways, supported me in the work with this thesis. My special thanks go to:

Professor Anders Hemmingsson, Head of the Department of Oncology, Radiology and Clinical Immunology, for creating a positive research atmosphere, showing continuous interest and all support;

Professor PG Lindgren, Head of the Department of Radiology, for employing me at the department and for all support;

Associate Professor Håkan Ahlström, my tutor, for kind provision of all necessary conditions for me to pursue this project, for always taking time, for prompt and thorough manuscript revisions, many rewarding discussions and

good company on ISMRM trips;

Associate Professor Anders Ericsson, my co-tutor, for sharing his wisdom on MRI physics and co-authorship in study IV;

Lars Johansson, for fruitful discussions on many aspects of MRI and for many good laughs!

Professor Örjan Smedby for co-authorship and invaluable statistical support;

Associate Professor Sadettin Karacagil, for committed co-authorship and sharing his knowledge on vascular surgery and duplex ultrasound scanning;

Ann-Marie Löfberg, Anders Holmberg, Miles Kirchin, Massimo Daprà, Hans-Rainer Hentrich, Martin Wasser, Peter Pattynama, Alberto Spinazzi, Arve Börseth and Per Åkeson, for co-authorship;

Alf Johansson, my mentor at the radiology department of Hudiksvall hospital, for being an excellent role model in terms of critical reasoning and humbleness and for sharing his interventional skills;

Anders Persson, head of the radiology department at Hudiksvall hospital, for generating a creative atmosphere, giving me insights into post-processing and for a positive attitude towards my PhD studies;

Olle Palmquist, former head of the department, who has taught me so much radiology, Karin Rydahl, my resident partner and friend, who kindly permitted numerous leaves of absence, Björn Relefors, for a rewarding, albeit too short, companionship at the MR unit and all other Hudiksvall colleagues for pleasant co-operation over the years and for putting up with a colleague that due to family and research commitments at times was an infrequent guest;

Britt-Marie Bolinder, Lillemor Lundström, Eva Näslund, Anders Lundberg and all other nurses at the MR unit, for skilful work throughout all the projects, enjoyable co-operation and for patience during my first stumbling steps into the world of MRI;

Nora Velastegui-Pettersson and Håkan Pettersson, for prompt and skilful assistance with numerous images, slides and posters during the last years, and for invaluable assistance with the thesis layout;

Tomas Bjerner, my PhD student colleague and friend, for all help on computer-related topics and for many rewarding discussions;

Christl Richter-Frohm for all support on financial and secretarial matters over the years;

Maud Marsden, for thorough and prompt linguistic advise;

Pirjo Jääskeläinen for kind assistance with searches in the data files;

Monika Gelotte for helping me keep track of piles of film sheets in study I;

Görel Östholm, for keeping track of the patients in study III;

Monika Winbäck, librarian at Hudiksvall hospital, for supplying numerous references;

Associate Professor Johan Bring, my neighbour, for kind advise on statistical matters;

Gävleborg county research council, for financial support;

Present colleagues at the section of neuroradiology for patience with a seldom present new member of the team;

Margareta and Folke Mellgren, my parents-in-law, for all support to my wife and children during my travels to Uppsala. This had not been possible without you!

Caisa and Lars Wikström, my parents, for a good upbringing and early encouragement of intellectual activities;

Last, but certainly not least, I am grateful to my wife, Anna-Karin, for all love and support. With clear-sighted knowledge of my personality she has encouraged these studies despite my other commitments. My absentmindedness may hopefully now reach a more bearable level!

REFERENCES

1. Missouris CG, Buckenham T, Cappuccio FP, MacGregor GA. Renal artery stenosis: a common and important problem in patients with peripheral vascular disease. Am J Med 1994;96(1):10-4.
2. Missouris CG, Papavassiliou MB, Khaw K, Hall T, Belli AM, Buckenham T, et al. High prevalence of carotid artery disease in patients with atheromatous renal artery stenosis. Nephrol Dial Transplant 1998;13(4):945-8.
3. May AG, de Weese JA, Rob CG. Hemodynamic effects of arterial stenosis. Surgery 1963;53(4):513-524.
4. Rauch U, Osende JI, Fuster V, Badimon JJ, Fayad Z, Chesebro JH. Thrombus Formation on Atherosclerotic Plaques: Pathogenesis and Clinical Consequences. Ann Intern Med 2001;134(3):224-238.
5. Berberich J, Hirsch S. Die roentgenographische Darstellung der Arterien und Venen am lebenden Menschen. Klinische Wochenschrift 1923:2226-2228.
6. Brooks B. Intra-arterial injection of sodium iodide. JAMA 1924;82:1016-1019.
7. Waugh JR, Sacharias N. Arteriographic complications in the DSA era. Radiology 1992;182(1):243-6.
8. Harrison D, Ricciardello M, Collins L. Evaluation of radiation dose and risk to the patient from coronary angiography. Aust N Z J Med 1998;28(5):597-603.
9. Smart RC. What are the risks of diagnostic medical radiation? Med J Aust 1997;166(11):589-91.
10. Katzberg RW. Urography into the 21st century: new contrast media, renal handling, imaging

characteristics, and nephrotoxicity. Radiology 1997;204(2):297-312.
11. May AG, van de Berg L, de Weese JA, Rob CG. Critical arterial stenosis. Surgery 1963;54(1):250-259.
12. Udoff EJ, Barth KH, Harrington DP, Kaufman SL, White RI. Hemodynamic significance of iliac artery stenosis: pressure measurements during angiography. Radiology 1979;132(2):289-93.
13. Castaneda-Zuniga W, Knight L, Formanek A, Moore R, D'Souza V, Amplatz K. Hemodynamic assessment of obstructive aortoiliac disease. Am J Roentgenol 1976;127(4):559-61.
14. Kinney TB, Rose SC. Intraarterial pressure measurements during angiographic evaluation of peripheral vascular disease: techniques, interpretation, applications, and limitations. AJR Am J Roentgenol 1996;166(2):277-84.
15. Flanigan DP, Ryan TJ, Williams LR, Schwartz JA, Gray B, Schuler JJ. Aortofemoral or femoropopliteal revascularization? A prospective evaluation of the papaverine test. J Vasc Surg 1984;1(1):215-23.
16. Brewster DC, Waltman AC, O'Hara PJ, Darling RC. Femoral artery pressure measurement during aortography. Circulation 1979;60(2 Pt 2):120-4.
17. Prokop M. Multislice CT angiography. Eur J Radiol 2000;36(2):86-96.
18. Link J, Mueller-Huelsbeck S, Brossmann J, Grabener M, Stock U, Heller M. Prospective assessment of carotid bifurcation disease with spiral CT angiography in surface shaded display (SSD)-technique. Comput Med Imaging Graph 1995;19(6):451-6.
19. Anderson GB, Findlay JM, Steinke DE, Ashforth R. Experience with computed tomographic angiography for the detection of intracranial aneurysms in the setting of acute subarachnoid hemorrhage. Neurosurgery 1997;41(3):522-7; discussion 527-8.
20. Rieker O, Duber C, Neufang A, Pitton M, Schweden F, Thelen M. CT angiography versus intraarterial digital subtraction angiography for assessment of aortoiliac occlusive disease. AJR Am J Roentgenol 1997;169(4):1133-8.
21. Prokop M. CT angiography of the abdominal arteries. Abdom Imaging 1998;23(5):462-8.
22. Calhoun PS, Kuszyk BS, Heath DG, Carley JC, Fishman EK. Three-dimensional volume rendering of spiral CT data: theory and method. Radiographics 1999;19(3):745-64.
23. Ranke C, Creutzig A, Alexander K. Duplex scanning of the peripheral arteries: correlation of the peak velocity ratio with angiographic diameter reduction. Ultrasound Med Biol 1992;18(5):433-40.
24. Legemate DA, Teeuwen C, Hoeneveld H, Eikelboom BC. Value of duplex scanning compared with angiography and pressure measurement in the assessment of aortoiliac arterial lesions. Br J Surg 1991;78(8):1003-8.
25. Stark DD, Bradley WG. Magnetic resonance imaging. Third ed. St. Louis: Mosby; 1999.
26. Johansson LO, Ahlstrom HK. Correlation between dose rate and T1 in blood at Gd-enhanced MR angiography. Acta Radiol 1998;39(5):579-82.
27. Prince M, Grist T, Debatin JF. 3D contrast MR angiography. 2nd ed: Springer-Verlag; 1999.
28. Kouwenhoven M. Contrast-enhanced MR angiography. Methods, limitations and possibilities. Acta Radiol Suppl 1997;412:57-67.
29. Prince MR. Gadolinium-enhanced MR aortography. Radiology 1994;191(1):155-64.
30. Snidow JJ, Aisen AM, Harris VJ, Trerotola SO, Johnson MS, Sawchuk AP, et al. Iliac artery MR angiography: comparison of three-dimensional gadolinium- enhanced and two-dimensional time-of-flight techniques. Radiology 1995;196(2):371-8.
31. Poon E, Yucel EK, Pagan-Marin H, Kayne H. Iliac artery stenosis measurements: comparison of two-dimensional time- of-flight and three-dimensional dynamic gadolinium-enhanced MR angiography. AJR Am J Roentgenol 1997;169(4):1139-44.
32. Willig DS, Turski PA, Frayne R, Graves VB, Korosec FR, Swan JS, et al. Contrast-enhanced 3D MR DSA of the carotid artery bifurcation: preliminary study of comparison with unenhanced 2D and 3D time-of- flight MR angiography. Radiology 1998;208(2):447-51.
33. Sardanelli F, Zandrino F, Parodi RC, De Caro G. MR angiography of internal carotid arteries: breath-hold Gd-enhanced 3D fast imaging with steady-state precession versus unenhanced 2D and 3D time-of-flight techniques. J Comput Assist Tomogr 1999;23(2):208-15.
34. Prince MR, Narasimham DL, Stanley JC, Wakefield TW, Messina LM, Zelenock GB, et al. Gadolinium-enhanced magnetic resonance angiography of abdominal aortic aneurysms. J Vasc Surg 1995;21(4):656-69.
35. Prince MR, Narasimham DL, Stanley JC, Chenevert TL, Williams DM, Marx MV, et al. Breath-hold gadolinium-enhanced MR angiography of the abdominal aorta and its major branches. Radiology 1995;197(3):785-92.
36. Prince MR, Narasimham DL, Jacoby WT, Williams DM, Cho KJ, Marx MV, et al. Three-dimensional gadolinium-enhanced MR angiography of the thoracic aorta. AJR Am J Roentgenol 1996;166(6):1387-97.
37. Steiner P, McKinnon GC, Romanowski B, Goehde SC, Hany T, Debatin JF. Contrast-enhanced, ultrafast 3D pulmonary MR angiography in a single

breath-hold: initial assessment of imaging performance. J Magn Reson Imaging 1997;7(1):177-82.
38. Hany TF, Debatin JF, Leung DA, Pfammatter T. Evaluation of the aortoiliac and renal arteries: comparison of breath- hold, contrast-enhanced, three-dimensional MR angiography with conventional catheter angiography. Radiology 1997;204(2):357-62.
39. Hany TF, Schmidt M, Schoenenberger AW, Debatin JF. Contrast-enhanced three-dimensional magnetic resonance angiography of the splanchnic vasculature before and after caloric stimulation. Original investigation. Invest Radiol 1998;33(9):682-6.
40. Snidow JJ, Johnson MS, Harris VJ, Margosian PM, Aisen AM, Lalka SG, et al. Three-dimensional gadolinium-enhanced MR angiography for aortoiliac inflow assessment plus renal artery screening in a single breath hold. Radiology 1996;198(3):725-32.
41. Parker DL, Tsuruda JS, Goodrich KC, Alexander AL, Buswell HR. Contrast-enhanced magnetic resonance angiography of cerebral arteries. A review. Invest Radiol 1998;33(9):560-72.
42. Lorenz CH, Johansson LO. Contrast-enhanced coronary MRA. J Magn Reson Imaging 1999;10(5):703-8.
43. Leclerc X, Gauvrit JY, Nicol L, Pruvo JP. Contrast-enhanced MR angiography of the craniocervical vessels: a review. Neuroradiology 1999;41(12):867-74.
44. de Haen C, Cabrini M, Akhnana L, Ratti D, Calabi L, Gozzini L. Gadobenate dimeglumine 0.5 M solution for injection (MultiHance) pharmaceutical formulation and physicochemical properties of a new magnetic resonance imaging contrast medium. J Comput Assist Tomogr 1999;23 Suppl 1:S161-8.
45. Spinazzi A, Lorusso V, Pirovano G, Kirchin M. Safety, tolerance, biodistribution, and MR imaging enhancement of the liver with gadobenate dimeglumine: results of clinical pharmacologic and pilot imaging studies in nonpatient and patient volunteers. Acad Radiol 1999;6(5):282-91.
46. Runge VM. Safety of approved MR contrast media for intravenous injection. J Magn Reson Imaging 2000;12(2):205-13.
47. Saeed M, Wendland MF, Higgins CB. Blood pool MR contrast agents for cardiovascular imaging. J Magn Reson Imaging 2000;12(6):890-8.
48. Weissleder R, Elizondo G, Wittenberg J, Rabito CA, Bengele HH, Josephson L. Ultrasmall superparamagnetic iron oxide: characterization of a new class of contrast agents for MR imaging. Radiology 1990;175(2):489-93.
49. Weissleder R, Elizondo G, Wittenberg J, Lee AS, Josephson L, Brady TJ. Ultrasmall superparamagnetic iron oxide: an intravenous contrast agent for assessing lymph nodes with MR imaging. Radiology 1990;175(2):494-8.
50. Saini S, Stark DD, Hahn PF, Bousquet JC, Introcasso J, Wittenberg J, et al. Ferrite particles: a superparamagnetic MR contrast agent for enhanced detection of liver carcinoma. Radiology 1987;162(1 Pt 1):217-22.
51. Saini S, Stark DD, Hahn PF, Wittenberg J, Brady TJ, Ferrucci JT. Ferrite particles: a superparamagnetic MR contrast agent for the reticuloendothelial system. Radiology 1987;162(1 Pt 1):211-6.
52. Mergo PJ, Helmberger T, Nicolas AI, Ros PR. Ring enhancement in ultrasmall superparamagnetic iron oxide MR imaging: a potential new sign for characterization of liver lesions. AJR Am J Roentgenol 1996;166(2):379-84.
53. Harisinghani MG, Saini S, Weissleder R, Halpern EF, Schima W, Rubin DL, et al. Differentiation of liver hemangiomas from metastases and hepatocellular carcinoma at MR imaging enhanced with blood-pool contrast agent Code- 7227. Radiology 1997;202(3):687-91.
54. Harisinghani MG, Saini S, Weissleder R, Hahn PF, Yantiss RK, Tempany C, et al. MR lymphangiography using ultrasmall superparamagnetic iron oxide in patients with primary abdominal and pelvic malignancies: radiographic- pathologic correlation. AJR Am J Roentgenol 1999;172(5):1347-51.
55. Chambon C, Clement O, Le Blanche A, Schouman-Claeys E, Frija G. Superparamagnetic iron oxides as positive MR contrast agents: in vitro and in vivo evidence. Magn Reson Imaging 1993;11(4):509-19.
56. Frank H, Weissleder R, Brady TJ. Enhancement of MR angiography with iron oxide: preliminary studies in whole-blood phantom and in animals. AJR Am J Roentgenol 1994;162(1):209-13.
57. Mayo-Smith WW, Saini S, Slater G, Kaufman JA, Sharma P, Hahn PF. MR contrast material for vascular enhancement: value of superparamagnetic iron oxide. AJR Am J Roentgenol 1996;166(1):73-7.
58. Knollmann FD, Bock JC, Teltenkotter S, Wlodarczyk W, Muhler A, Vogl TJ, et al. Evaluation of portal MR angiography using superparamagnetic iron oxide. J Magn Reson Imaging 1997;7(1):191-6.
59. Stillman AE, Wilke N, Li D, Haacke M, McLachlan S. Ultrasmall superparamagnetic iron oxide to enhance MRA of the renal and coronary arteries: studies in human patients. J Comput Assist Tomogr 1996;20(1):51-5.
60. Anzai Y, Prince MR, Chenevert TL, Maki JH, Londy F, London M, et al. MR angiography with an ultrasmall superparamagnetic iron oxide blood pool agent. J Magn Reson Imaging 1997;7(1):209-14.
61. Bjornerud A, Wendland MF, Johansson L, Ahlstrom HK, Higgins CB, Oksendal A. Use of intra-

vascular contrast agents in MRI. Acad Radiol 1998;5 Suppl 1:S223-5.
62. Earls JP, Rofsky NM, DeCorato DR, Krinsky GA, Weinreb JC. Hepatic arterial-phase dynamic gadolinium-enhanced MR imaging: optimization with a test examination and a power injector. Radiology 1997;202(1):268-73.
63. Kim JK, Farb RI, Wright GA. Test bolus examination in the carotid artery at dynamic gadolinium- enhanced MR angiography. Radiology 1998;206(1):283-9.
64. Foo TK, Saranathan M, Prince MR, Chenevert TL. Automated detection of bolus arrival and initiation of data acquisition in fast, three-dimensional, gadolinium-enhanced MR angiography. Radiology 1997;203(1):275-80.
65. Wilman AH, Riederer SJ, King BF, Debbins JP, Rossman PJ, Ehman RL. Fluoroscopically triggered contrast-enhanced three-dimensional MR angiography with elliptical centric view order: application to the renal arteries. Radiology 1997;205(1):137-46.
66. Levy RA, Maki JH. Three-dimensional contrast-enhanced MR angiography of the extracranial carotid arteries: two techniques. AJNR Am J Neuroradiol 1998;19(4):688-90.
67. Golledge J. Lower-limb arterial disease. Lancet 1997;350(9089):1459-65.
68. Currie IC, Jones AJ, Wakeley CJ, Tennant WG, Wilson YG, Baird RN, et al. Non-invasive aortoiliac assessment. Eur J Vasc Endovasc Surg 1995;9(1):24-8.
69. Ho KY, Leiner T, de Haan MW, Kessels AG, Kitslaar PJ, van Engelshoven JM. Peripheral vascular tree stenoses: evaluation with moving-bed infusion- tracking MR angiography. Radiology 1998;206(3):683-92.
70. Rofsky NM, Johnson G, Adelman MA, Rosen RJ, Krinsky GA, Weinreb JC. Peripheral vascular disease evaluated with reduced-dose gadolinium-enhanced MR angiography. Radiology 1997;205(1):163-9.
71. Meaney JF, Ridgway JP, Chakraverty S, Robertson I, Kessel D, Radjenovic A, et al. Stepping-table gadolinium-enhanced digital subtraction MR angiography of the aorta and lower extremity arteries: preliminary experience. Radiology 1999;211(1):59-67.
72. Anderson CM, Saloner D, Tsuruda JS, Shapeero LG, Lee RE. Artifacts in maximum-intensity-projection display of MR angiograms. AJR Am J Roentgenol 1990;154(3):623-9.
73. Davis CP, Hany TF, Wildermuth S, Schmidt M, Debatin JF. Postprocessing techniques for gadolinium-enhanced three-dimensional MR angiography. Radiographics 1997;17(5):1061-77.
74. Seldinger SI. Catheter replacement of the needle in percutaneous angiography. Acta Radiol 1953;39:368-376.
75. Bishop VMM, Fienberg SE, Holland PW. Discrete multivariate analysis. Cambridge, Mass.: M.I.T. Press; 1975.
76. Colton T. Statistics in medicine. Boston, Mass.; 1974.
77. van der Meulen P, Groen JP, Tinus AM, Bruntink G. Fast Field Echo imaging: an overview and contrast calculations. Magn Reson Imaging 1988;6(4):355-68.
78. Flanigan DP, Tullis JP, Streeter VL, Whitehouse WM, Fry WJ, Stanley JC. Multiple subcritical arterial stenoses: effect on poststenotic pressure and flow. Ann Surg 1977;186(5):663-8.
79. Grollman JH, Marcus R, Averbook BD, Fiaschetti FL. Bilateral aortoiliac pressure measurements from a single puncture site. Cardiovasc Intervent Radiol 1990;13(6):367-71.
80. Leiboff R, Bren G, Katz R, Korkegi R, Ross A. Determinants of transstenotic gradients observed during angioplasty: an experimental model. Am J Cardiol 1983;52(10):1311-7.
81. McWilliams RG, Robertson I, Smye SW, Wijesinghe L, Kessel D. Sources of error in intra-arterial pressure measurements across a stenosis. Eur J Vasc Endovasc Surg 1998;15(6):535-40.
82. Legemate DA, Teeuwen C, Hoeneveld H, Eikelboom BC. How can the assessment of the hemodynamic significance of aortoiliac arterial stenosis by duplex scanning be improved? A comparative study with intraarterial pressure measurement. J Vasc Surg 1993;17(4):676-84.
83. Mohiaddin RH, Sampson C, Firmin DN, Longmore DB. Magnetic resonance morphological, chemical shift and flow imaging in peripheral vascular disease. Eur J Vasc Surg 1991;5(4):383-96.
84. Schoenberg SO, Knopp MV, Bock M, Kallinowski F, Just A, Essig M, et al. Renal artery stenosis: grading of hemodynamic changes with cine phase-contrast MR blood flow measurements. Radiology 1997;203(1):45-53.
85. Maki JH, Prince MR, Londy FJ, Chenevert TL. The effects of time varying intravascular signal intensity and k-space acquisition order on three-dimensional MR angiography image quality. J Magn Reson Imaging 1996;6(4):642-51.
86. Svensson J, Petersson JS, Stahlberg F, Larsson EM, Leander P, Olsson LE. Image artifacts due to a time-varying contrast medium concentration in 3D contrast-enhanced MRA. J Magn Reson Imaging 1999;10(6):919-28.
87. Korosec FR, Frayne R, Grist TM, Mistretta CA. Time-resolved contrast-enhanced 3D MR angiogra-

phy. Magn Reson Med 1996;36(3):345-51.
88. Claussen CD, Banzer D, Pfretzschner C, Kalender WA, Schorner W. Bolus geometry and dynamics after intravenous contrast medium injection. Radiology 1984;153(2):365-8.
89. Corot C, Violas X, Robert P, Port M. Pharmacokinetics of three gadolinium chelates with different molecular sizes shortly after intravenous injection in rabbits: relevance to MR angiography. Invest Radiol 2000;35(4):213-8.
90. Knopp MV, von Tengg-Kobligk H, Floemer F, Schoenberg SO. Contrast agents for MRA: future directions. J Magn Reson Imaging 1999;10(3):314-6.
91. Knopp MV, Schoenberg SO, Rehm C, Bock M, Essig M, Floemer F, et al. Assessment of a weakly binding Gd-chelate (Gd-BOPTA) for MR-angiography: results of phase I studies. In: 15th annual meeting ESMRMB; 1998; Geneva, Switzerland; 1998. p. 85.
92. Knopp MV, Schoenberg SO, Rehm C, Bock M, Essig M, Floemer F, et al. Comparison of the efficacy of Gd-BOPTA and Gd-DTPA for MR Angiography: A Phase I Pilot Study. In: Sixth Scientific Meeting and Exhibition; 1998; Sydney, Australia: International Society for Magnetic Resonance in Medicine; 1998. p. 174.
93. Elgersma OE, Wust AF, Buijs PC, van Der Graaf Y, Eikelboom BC, Mali WP. Multidirectional depiction of internal carotid arterial stenosis: three-dimensional time-of-flight MR angiography versus rotational and conventional digital subtraction angiography. Radiology 2000;216(2):511-6.
94. Cavagna FM, Maggioni F, Castelli PM, Dapra M, Imperatori LG, Lorusso V, et al. Gadolinium chelates with weak binding to serum proteins. A new class of high-efficiency, general purpose contrast agents for magnetic resonance imaging. Invest Radiol 1997;32(12):780-96.
95. Kroft LJ, de Roos A. Blood pool contrast agents for cardiovascular MR imaging. J Magn Reson Imaging 1999;10(3):395-403.
96. Engelbrecht MR, Saeed M, Wendland MF, Canet E, Oksendal AN, Higgins CB. Contrast-enhanced 3D-TOF MRA of peripheral vessels: intravascular versus extracellular MR contrast media. J Magn Reson Imaging 1998;8(3):616-21.
97. Bjornerud A, Briley-Saebo K, Johansson LO, Kellar KE. Effect of NC100150 injection on the (1)H NMR linewidth of human whole blood ex vivo: dependency on blood oxygen tension. Magn Reson Med 2000;44(5):803-7.
98. Ahlstrom KH, Johansson LO, Rodenburg JB, Ragnarsson AS, Akeson P, Borseth A. Pulmonary MR angiography with ultrasmall superparamagnetic iron oxide particles as a blood pool agent and a navigator echo for respiratory gating: pilot study. Radiology 1999;211(3):865-9.
99. Pan XM, Saloner D, Reilly LM, Bowersox JC, Murray SP, Anderson CM, et al. Assessment of carotid artery stenosis by ultrasonography, conventional angiography, and magnetic resonance angiography: correlation with ex vivo measurement of plaque stenosis. J Vasc Surg 1995;21(1):82-8; discussion 88-9.
100. Laub G. Displays for MR angiography. Magn Reson Med 1990;14(2):222-9.
101. Verhoek G, Costello P, Khoo EW, Wu R, Kat E, Fitridge RA. Carotid bifurcation CT angiography: assessment of interactive volume rendering. J Comput Assist Tomogr 1999;23(4):590-6.
102. Eberhardt KE, Tomandl B, Nomayr A, Huk WJ. [Value of CT-angiography in the diagnosis of cerebral artery aneurysms]. Radiologe 1997;37(11):905-12.
103. Wang Y, Yu Y, Li D, Bae KT, Brown JJ, Lin W, et al. Artery and vein separation using susceptibility-dependent phase in contrast-enhanced MRA. J Magn Reson Imaging 2000;12(5):661-70.
104. Smedby Ö, Svensson S, Löfstrand T. Greyscale connectivity concept for visualizing MRA and CTA volumes. Proceedings of the SPIE 1999; 3658:212-219.
105. Fayad ZA, Fuster V. Characterization of atherosclerotic plaques by magnetic resonance imaging. Ann N Y Acad Sci 2000;902:173-86.